Separation and Purification Technology 357 (2025) 130059

Contents lists available at ScienceDirect

Separation and Purification Technology

journal homepage: www.elsevier.com/locate/seppur

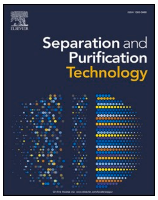

Review

MOFs-coupled fiber membranes: A versatile platform for water purification

Jingwen Chang, Ye Bian *, Yong Wang *

School of Energy and Environment, Southeast University, Nanjing 210096, China

ARTICLE INFO

Editor: Gaohong He

Keywords:
Metal-organic frameworks
Fiber substrate
MOFs-coupled-fiber membranes
Water purification
Membrane-based purification

ABSTRACT

Due to the high chemical and structural diversity, metal-organic frameworks (MOFs) have attracted great interest in water purification. However, the poor processability of MOF powders has hindered their practical applications. To achieve the efficient utilization of MOFs during water treatment, it is effective to combine MOFs with flexible fiber substrates into composite membranes. In this review, the research progress of rational development strategies of MOFs-coupled-fiber membranes was summarized, divided by the formation of MOFs. Furthermore, the pros and cons of different techniques for the synthesis of MOFs-coupled-fiber membranes were elaborated. Based on the understanding of the synthesis strategies, the applications of MOFs-coupled-fiber membranes for the removal of waterborne contaminants were listed, including heavy metal ions, organic dyes, and emerging pollutants. The purification performance largely depends on the structure of MOFs-coupled-fiber membranes and, ultimately on the synthesis strategies. To uncover the full potential of MOFs-coupled-fiber membranes in practical applications, current challenges and perspectives were also proposed. This review aims to help researchers gain a deep understanding of the important effect of MOFs-coupled-fiber membranes in wastewater treatment and provide theoretical guidance for the design and development of functional membranes.

Abbreviations	
MOFs	Metal-organic frameworks
LbL	Layer-by-layer
HoP	Hot pressing
ALD	Atomic layer deposition
AOP	Advanced oxidation process
DMF	*N, N*-dimethylformamide
2-MI	2-methylimidazole
MIM	1-methylimidazole
PAN	Polyacrylonitrile
PVDF	Polyvinylidene fluoride
PS	Polystyrene
PST	P(St-*co*-TMSPMA)
PLA	Polylactic acid
PP	Polypropylene
PBT	Polybutylene terephthalate
PVP	Polyvinyl pyrrolidone
PVA	Polyvinyl alcohol
PFOA	Perfluorooctanoic acid
CFC	Carbon fiber cloth
CA	Cellulose acetate
RhB	Rhodamine B
EPs	Emerging pollutants
POPs	Persistent organic pollutants
PMS	Peroxymonosulfate

1. Introduction

Water is an essential resource for the survival of all the livings on the earth. Clean and sustainable freshwater is a basic requirement for people's daily lives and industrial activities. However, the shortage of freshwater resources remains a huge threat to humans. The World Health Organization anticipated that water shortage may affect up to 1.9 billion people by 2030 [1]. In addition, with the acceleration of population growth and industrialization development, a large amount of wastewater has been discharged into natural water bodies, which may damage their self-cleaning ability and exacerbate water shortage [2]. More importantly, sewage contains a series of pollutants, including organic dyes, heavy metal ions, drugs, antibiotics, etc. [3–5], which could introduce waterborne diseases, further causing serious health problems for humans. Therefore, it is significant to develop efficient technologies for water purification.

The membrane is defined as a semi-permeable barrier between two phases [6]. Membrane-based water purification is a complex process including membrane filtration, adsorption, and catalytic degradation.

---

* Corresponding authors.
E-mail addresses: yebian@seu.edu.cn (Y. Bian), yongwang@seu.edu.cn (Y. Wang).

https://doi.org/10.1016/j.seppur.2024.130059
Received 26 July 2024; Received in revised form 29 September 2024; Accepted 8 October 2024

However, traditional membranes face the disadvantages of low efficiency, lack of durability and reusability, etc., which limit their application in the field of water purification [7–10]. Therefore, it is necessary to develop functional membranes to remove pollutants from water bodies effectively. Combining functional materials with membranes can significantly enhance the purification of waterborne pollutants. Among various functional materials, metal–organic frameworks (MOFs) have emerged as promising candidates for water purification [11]. MOFs are a class of porous materials composed of metal ions or metal clusters connected by organic ligands, which achieve highly ordered structures and adjustable pore sizes [12–14]. Due to the porous structure, abundant functional groups, and excellent physical–chemical properties, MOFs attain the ideal performance of high efficiency and reusability in the application of water purification [15]. To take full use of the strengths of MOFs, a series of substrates have been proposed to combine with MOF powders, including fiber, film, carbon nanotubes, foam, etc. [16–22] Among these hybrid materials, flexible fiber substrates can achieve effective loading performance of MOFs due to their relatively large specific surface area, high porosity, and structural tenability [23–27]. Different loading strategies have important effects on the structural characteristics of MOF fibers such as diameter and porosity, as well as the exposure of active sites of MOFs on the composite membranes, which in turn exhibit different purification performance in water treatment [28].

This review focused on the fiber substrate, summarizing recent progress in the development of MOFs-coupled-fiber membranes and their application in water purification. The categorization of composite fibrous membranes is based on the combination of MOFs and fibers, such as conventional solvothermal synthesis, unconventional synthesis of MOFs on fiber surfaces, and coupling pre-synthesized MOFs with fibers. Moreover, the influence of the structure of MOFs-coupled-fiber membranes on the control of waterborne contaminants was also systematically discussed. The main contents of this review are shown in Fig. 1. The review includes four parts: Introduction (Section 1), Preparation of MOFs-coupled-fiber membranes (Section 2), Applications of MOFs-coupled-fiber membranes in removing contaminants from water (Section 3) and Current challenges and future chances (Section 4). In Section 2, the preparation strategies of MOFs-coupled-fiber membranes are categorized into three subclasses based on the formation of MOFs, namely conventional solvothermal synthesis (including direct solvothermal growth and seed-assisted secondary growth), unconventional synthesis of MOFs on fiber surfaces (including solvent-free hot pressing method, layer-by-layer growth, and atomic-layer-deposition-assisted growth), and coupling pre-synthesized MOFs with fibers (including doping during electrospinning and covalent immobilization coating). Pros and cons of different preparation strategies are analyzed thoroughly based on the categorization. Section 3 is divided into 3 parts based on the type of waterborne contaminants. The application with the use of MOFs-coupled-fiber membranes for water treatment are discussed and analyzed in this section. Moreover, current challenges and future chances of MOFs-coupled-fiber membranes are put forward in Section 4. Critical factors in composite synthesis, innovation of characterization techniques, comprehensive design of devices, the practical application of MOFs-coupled-fiber membranes, and the related environmental risks are taken into consideration.

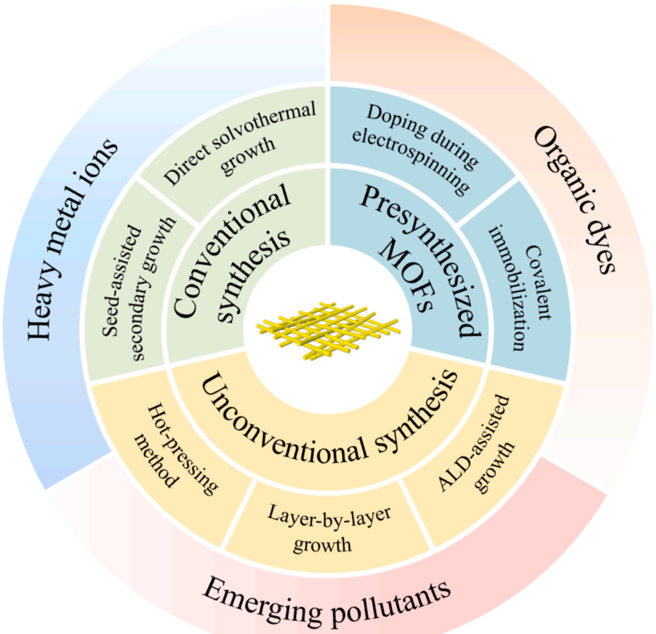

Fig. 1. General overview of preparation and application in water purification of MOFs-coupled-fiber membranes.

2. Preparation of MOFs-coupled-fiber membranes

MOFs have exhibited great promise in the application of water purification [23,29–33]. However, there also exist several drawbacks when MOFs are used in the form of powders, such as easy decomposition, poor reusability, secondary pollution, etc. [34–38] Anchoring MOFs on the substrates could overcome these drawbacks. Among various substrates, fiber-based membranes are one of the most popular candidates due to the strengths of large surface area, easy operation, and good extensibility [39–45]. The development of MOFs-coupled-fiber membranes is mainly achieved through three approaches based on the formation of MOFs, namely conventional solvothermal synthesis, unconventional synthesis of MOFs on fiber surfaces, and coupling pre-synthesized MOFs with fibers.

2.1. *Conventional solvothermal synthesis*

Solvothermal synthesis is a preferred method for the synthesis of MOFs-coupled-fiber membranes. In the solvent environment, MOF precursors can nucleate, crystallize, and grow on fibers, forming MOF-coupled-fibers with uniform MOFs coverage [46]. Two different structures of MOFs-coupled-fiber membranes could be generated through conventional solvothermal synthesis: MOF particles attached on the surface of fibers, and MOF particles partially-embedded into the fiber [47].

2.1.1. *Direct solvothermal growth*

Direct growth refers to submerging the substrate in a solution, where the processes of crystal nucleation and growth of MOFs on the substrate all occur in this stage as shown in Fig. 2**a**. During the process, MOFs crystallize on the surface of fibers. The direct solvothermal growth technique has been proven successful for several MOF types including ZIF, UiO, MIL, HKUST, etc. [48–56] There are several common substrates for solvothermal synthesis, such as carbon cloths, glass fibers, nonwoven electrospun fibers, etc. Carbon fiber cloth (CFC) is a substrate with satisfactory stability and mechanical strength [57,58]. However, it is not applicable for the direct use of CFC as the substrate during the solvothermal process due to the lack of bonding sites. To provide covalent bonding between CFC substrate and MOFs, the carboxyl group (–COOH) could be introduced on CFC with the aid of acetic acid [57]. Benefiting from the bonding between metal ions and –COOH, UiO-66-NH_2 particles grew firmly on the CFC surface with a relatively high MOF loading amount. Modifying surfaces with functional groups is also necessary for glass fibers to achieve a feasible combination between MOFs and glass fiber substrates. With the modification of polyaniline/chitosan on glass fiber, bimetallic MOF could well cover the surface of glass fiber with chopstick-like particles as shown in Fig. 2**b, c** [59]. The resultant fiber membranes displayed a high specific surface area, which

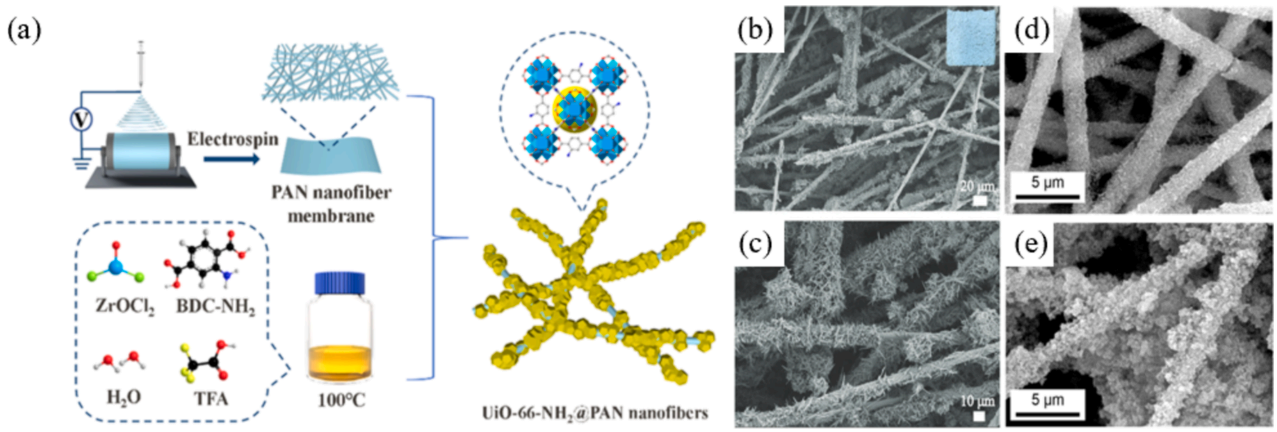

Fig. 2. (a) Illustrated diagram of the preparation of UiO-66-NH$_2$ fiber membranes[69]; (b, c) SEM images of bimetallic MOF fibers [59]; (d, e) SEM images of MIL-53(Al)-m1 and MIL-53(Al)-m3[61].

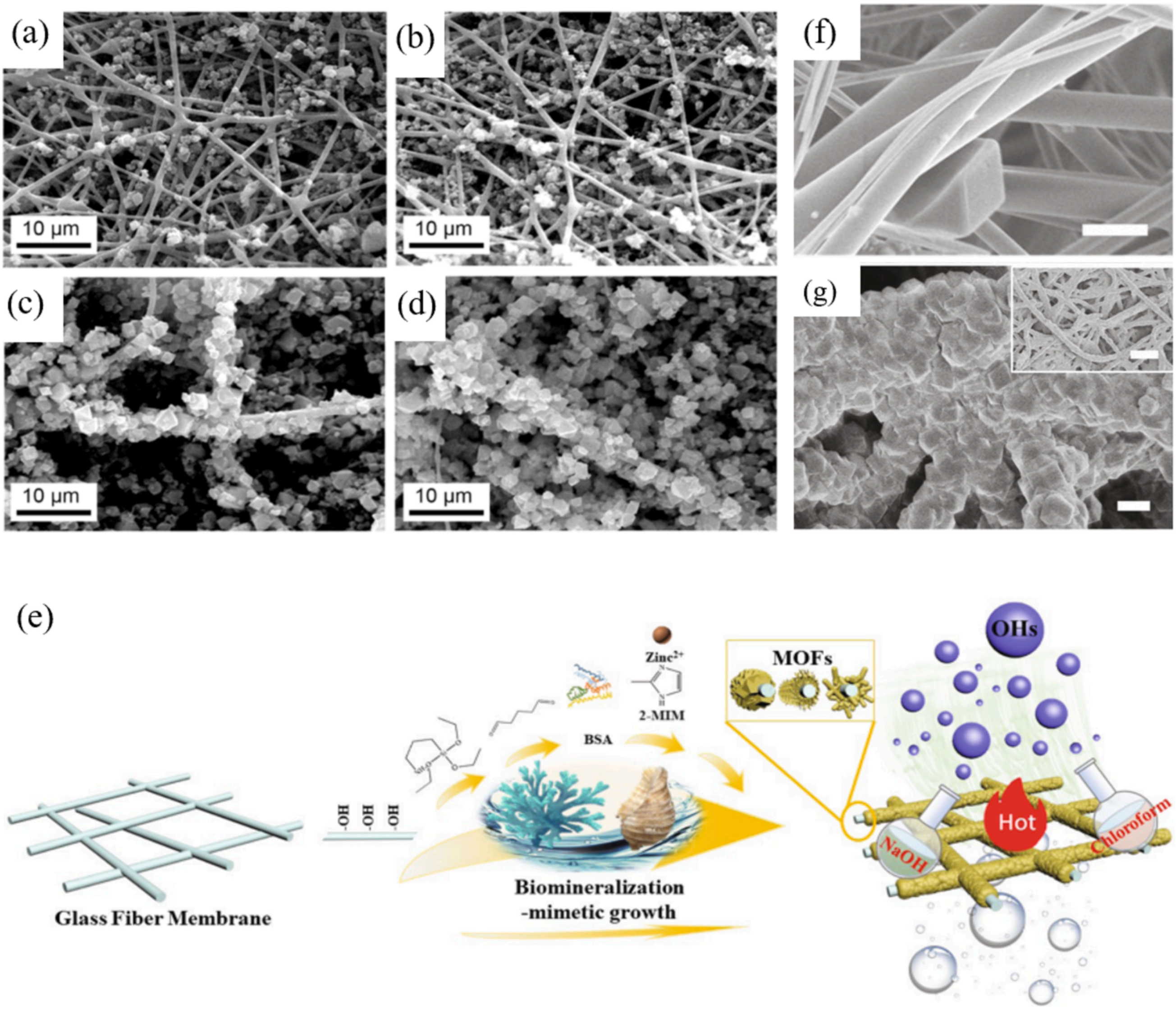

Fig. 3. SEM images of (a) HKUST-1-m1, (b) HKUST-1-m2, (c) HKUST-1-m3, (d) HKUST-1-m4 (the number following m refers to the repeating time of deposition procedure)[61]. (e) Illustration of the biomineralization-mimetic growth of GF@MOFs; (f) SEM image of GF-ZIF-8 fibers; (g) SEM image of GF-BSA@ZIF-8 fibers[72].

ensured promising performance in the control of pollutants. Furthermore, electrospun nanofibrous mats are ideal MOF-loading substrates due to their large specific surface area and easy-to-functionalize modification [60]. For example, Liu *et al.* [61] fabricated HKUST-1 and MIL-53(Al)-based fiber membranes through the solvothermal method with electrospun nanofiber substrate. Due to the fine regulation of electrospun fiber structures, the loading performance of MOFs can be well-adjusted accordingly. The SEM image (Fig. 2**d, e**) showed that both the particle size and quantity increased by repeating the solvothermal growth cycle.

The selection of solvents is crucial for electrospun fiber membranes during the formation process of MOFs-coupled-fiber membranes since some solvents could corrode polymer substrate materials [46]. For instance, *N, N*-dimethylformamide (DMF) is one of the typical solvents that could solubilize a series of polymer candidates such as polyacrylonitrile (PAN), polyvinylidene fluoride (PVDF), polystyrene (PS), etc. [62–67]. Therefore, solvents that are insoluble in polymer substrates need to be used during the solvothermal process. For example, when the electrospun fiber substrate is made of PAN, an insoluble solvent of acetone could enable the growth of UiO-66-NH_2 on an intact PAN nanofiber membrane [67]. In addition to acetone, deionized water is also a solvent choice for maintaining the integrity of the PAN fiber substrate [68]. Combined deionized water with trifluoroacetic acid (TFA), the growth velocity of MOF particles on fiber substrates could be modulated [69]. Ma *et al.* [70] applied a mixture of deionized water and TFA as the modulator during solvothermal synthesis to grow MOF-808/polyester fibers. During which, TFA was introduced to slow down the crystallization of MOF particles, resulting in an evenly distributed MOF coating on the surface of substrates.

Unfortunately, the drawback of the introduced strategy is that most of the MOF nucleation occurs in the solvent rather than on the fiber surface during the solvothermal process, which leads to a waste of reagents and a relatively low loading amount of MOFs [71]. To improve the loading amount, successive solvothermal reaction procedures could be adopted. A small portion of HKUST-1 particles were initially anchored on the surface of fibers. By repeating the reaction procedure, more crystals were observed on the nanofibers, and the space in the net structure was filled gradually with MOFs as shown in Fig. 3**a-d** [61]. In addition, a modified fiber surface with specific functional groups could facilitate the loading procedure. Biomineralization, a phenomenon derived from nature, could be applied to the growth of MOFs on glass fibers triggered by Bovine serum albumin (BSA), which is a type of biomolecule [72]. The available glass fibers were activated using the silylanization method to graft NH_2 groups, then glutaraldehyde was used to link BSA with NH_2 groups, introducing BSA to the fiber surface. Afterward, precursors of ZIF-8 were added, forming the ZIF-8@GF membrane (Fig. 3**e**). Compared with bare glass fibers, the coverage of MOFs on GF-BSA fibers was significantly high as shown in Fig. 3**f, g**. This could be attributed to the high density of BSA, which served as functional sites for the nucleation of MOFs. By adjusting the ratios of precursors, different morphologies of MOFs on the surface of glass fiber could be achieved. Likewise, Li *et al.* [73] proposed a biomineralization-mimetic method to prepare electrospun-silk-nanofiber@MOF membranes. Without the use of a biomineralization medium, the electrospun silk fibers were immersed in the solution containing one kind of precursor first, followed by the addition of the other kind of precursor to hybrid with MOFs, which could decrease the nucleation of MOFs in the solution. Due to the rich functional groups and complex biological entities, silk fibers had abundant active sites for the biomineralization growth of MOFs, resulting in fully covered hybrid fibers. Also, since the strong affinity between silk fibers and MI through hydrogen bonding and hydrophobic interactions, the connection between MOFs and fibers was stronger.

2.1.2. Seed-assisted secondary growth

Seed-assisted secondary growth refers to the growth of MOFs on a membrane in which the seed is previously attached [11]. In detail, MOF particles or precursors are embedded into substrates firstly, which is regarded as the seed. Afterward, the seeded substrate further reacts with the suspension containing the MOF precursors, during which crystallization proceeds as shown in Fig. 4**a**. It is advantageous in anchoring the points where MOFs grow and enhancing the loading amount of MOFs. The seed-assisted secondary growth method is widely cooperated with electrospinning technology. For example, Zhang *et al.* [74] fabricated HKUST-1/PAN nanofiber membranes through electrospinning and seed-assisted secondary growth. HKUST-1 particles were impregnated into PAN fibers as seeds. Subsequently, the seeded fiber was placed in an autoclave with the precursor solution of HKUST-1 and heated at 80 °C overnight for secondary solvothermal growth. Likewise, Zn-MOF/PST fibers were synthesized [75]. It is notable that for MOFs that could be synthesized under room temperature (e.g., ZIFs), the heating and pressure during secondary growth are unnecessary.

Apart from seeding with MOF particles, the selection of metal ions as seeds inside the substrates is widely used for the development of MOFs-coupled-fiber membranes. For example, ZIF-8 is a kind of MOF that can be synthesized under ambient temperature between the reaction of Zn ions and the organic linker of 2-methylimidazole (2-MI). Through seed-assisted secondary growth, ZIF-8@PAN nanofiber membranes could be well-constructed [76]. The seeded substrate containing Zn^{2+} was obtained using the electrospinning technique. Then the resultant substrate was immersed in a 2-MI solution, where the seeded Zn^{2+} reacted with the organic linker and ZIF-8 crystallized on the surface of the fibers. By altering the ratio of metal ions in polymeric substrates, the morphology and diameter of the developed MOF fibers could be regulated accordingly. Moreover, the loading of MOF particles forms a layer covering the surface of nanofibers, of which thickness can be tuned by controlling the concentration of metal ions inside the fiber [77]. Similarly, morphology and diameters of ZIF-67-based fibers could be controlled by altering the molar ratio of $Co(AC)_2$ to PAN in electrospun solutions from 80 wt% to 200 wt% [78]. With the increase of the molar ratio, the MOF particles covered on the surface of the fiber became homogeneous gradually, and the roughness of the fiber increased as well as shown in Fig. 4**b-d**. As seen in Fig. 4**e-g**, MOFs were partially-inserted into the fiber, which was an enhancement to the mechanical properties.

Seeding with organic ligands is also available. During the development of UiO-66-NH_2-based nanofiber, Lu *et al.* [67] selected the organic ligand of amino-terephthalic acid (ATA) as the nucleation point for MOF growth inside the fiber. Then the seeding fiber was submerged in the solution containing both Zr ions and ATA, which enabled the growth of UiO-66-NH_2 to continuously cover the fiber surface even at a low precursor concentration. Higher precursor concentrations could result in more homogeneous coverage and larger MOF clusters, and the MOF loading amount could achieve up to 50 % [67]. Seeding with organic ligands could also be advanced to form ZIF-8/PLA nanofiber mats [79]. The PLA nanofiber membrane with 2-MI seeds was first added into the Zn^{2+} solution to form a few ZIF-8 nanocrystals on the fiber surface, which served as the growth core. The core-nanofiber membranes were further added to a 2-MI aqueous solution, where the ZIF-8 particles grew larger. Also, more ZIF-8 particles can be anchored on the fiber surface with a prolonged nucleation time, enhancing the roughness and hydrophilicity of the membranes.

2.2. Unconventional synthesis of MOFs on fiber surfaces

Apart from conventional solvothermal synthesis, a series of peculiar methods could be applied to the fabrication of MOFs-coupled-fiber membranes. The hot pressing method, layer-by-layer growth method, and ALD-assisted growth method are representatives. The unconventional synthesis of MOFs-coupled-fiber membranes involves specific synthesis conditions and growth methods of MOFs on the fiber surface compared to conventional methods, such as solvent-free synthesis environments, multiple repetitions of dipping, the need for adequate

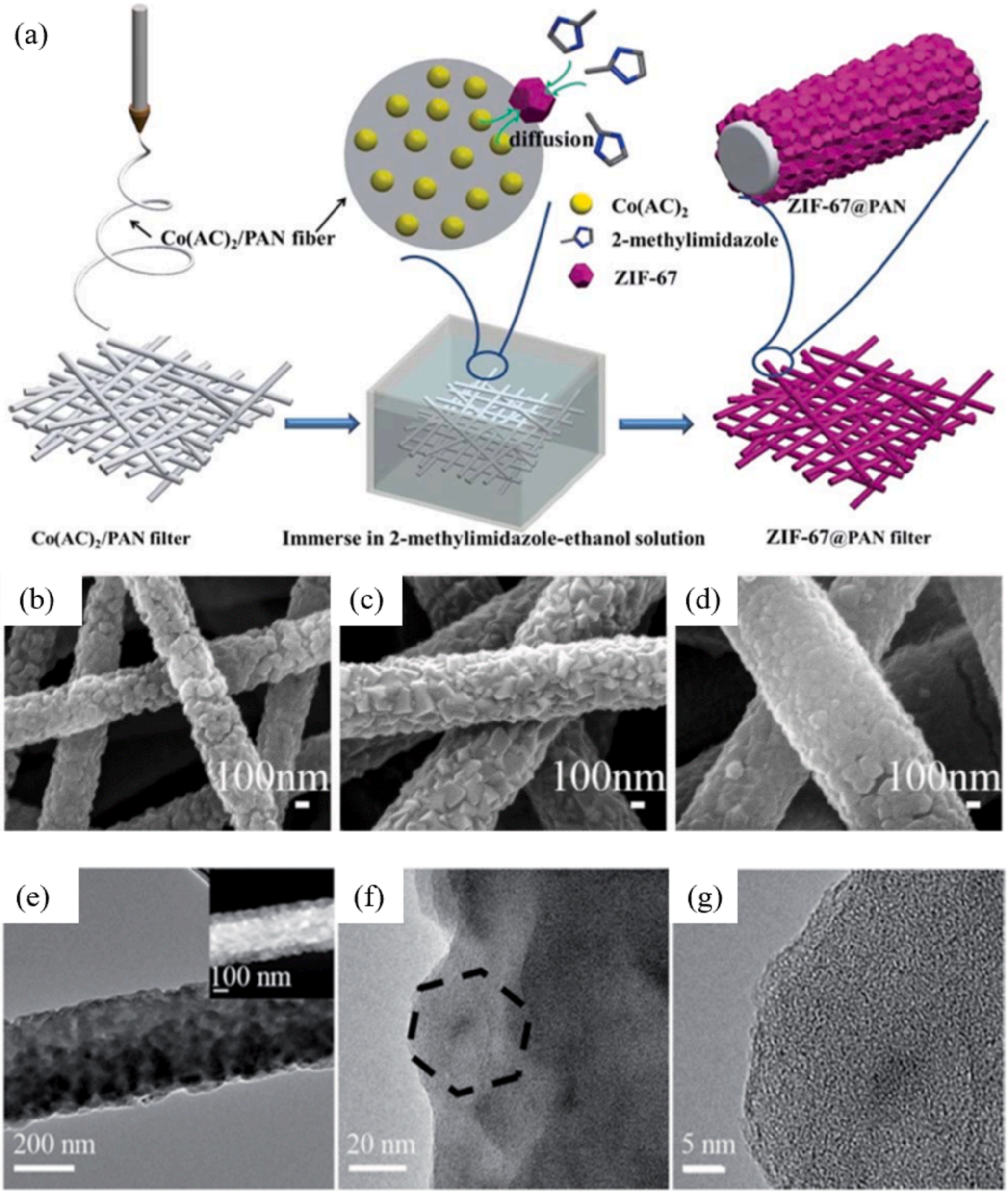

Fig. 4. (a) Schematic illustration of the ZIF-67-based nanofiber filter fabrication procedure. SEM images of ZIF-67@PAN composite electrospun fiber with the mass ratio of $Co(Ac)_2$ to PAN of (b) 160%, (c) 80%, and (d) 200%. (e) bright-field and dark-field TEM images of the ZIF-67@PAN filter; (f) and (g) high-resolution TEM images of the ZIF-67@PAN filter[78].

binding layers, etc.

2.2.1. *Solvent-free hot pressing method*

Recently, a solvent-free hot pressing (HoP) method has been reported to directly transfer MOF coatings on various substrates including plastic mesh, glass cloth, carbon cloth, metal mesh, nonwoven fabric, etc. [80,81] Generally, the MOF precursors are cast onto substrates and heated to produce MOFs-coupled-fiber membranes as shown in Fig. 5**a**. With increasing cycle times of casting and heating, the quantity of loaded MOFs increases accordingly [82]. Based on the traditional hot pressing method, a roll-to-roll method was presented for mass production of MOFs-coupled-fiber membranes, which is regarded as a large-scale fabrication strategy [80]. In the roll-to-roll process, the substrates covered by MOF precursors are rolled between two heated rollers as shown in Fig. 5**b**. After rolling back and forth several times, MOF nanocrystals are generated on the substrate fiber. The HoP method was applicable to a series of MOFs including Zn-MOF, Cu-MOF, Co-MOF, Cd-MOF, etc., and the obtained MOF membranes showed excellent robustness and brilliant performance in environmental application [83].

The heating temperature involved in the HoP process is essential for the dispersion of MOFs on the fiber substrate. Peng and co-workers [84] investigated the effect of heating temperatures on the development of ZIF-8-based electrospun fiber membrane, during which the precursors were loaded on PAN nanofibers and heated under desired working temperatures (from 80 to 140 °C). The most uniform growth of ZIF-8 nanoparticles on the surface of PAN fibers occurred when the working temperature was at 120 °C, while either weak crystallinity or slight agglomeration occurred. It is believed that relatively high temperature increases the possibility of molecular collision between ZIF-8 precursors, contributing to rapid crystallization. Excessively high temperatures may lead to large grains of ZIF-8 particles on PAN fibers, while the crystallization would be limited under low temperatures. Furthermore, changing the way of heating could optimize the development process of MOF fibers. Instead of using a traditional electric iron to heat one side of

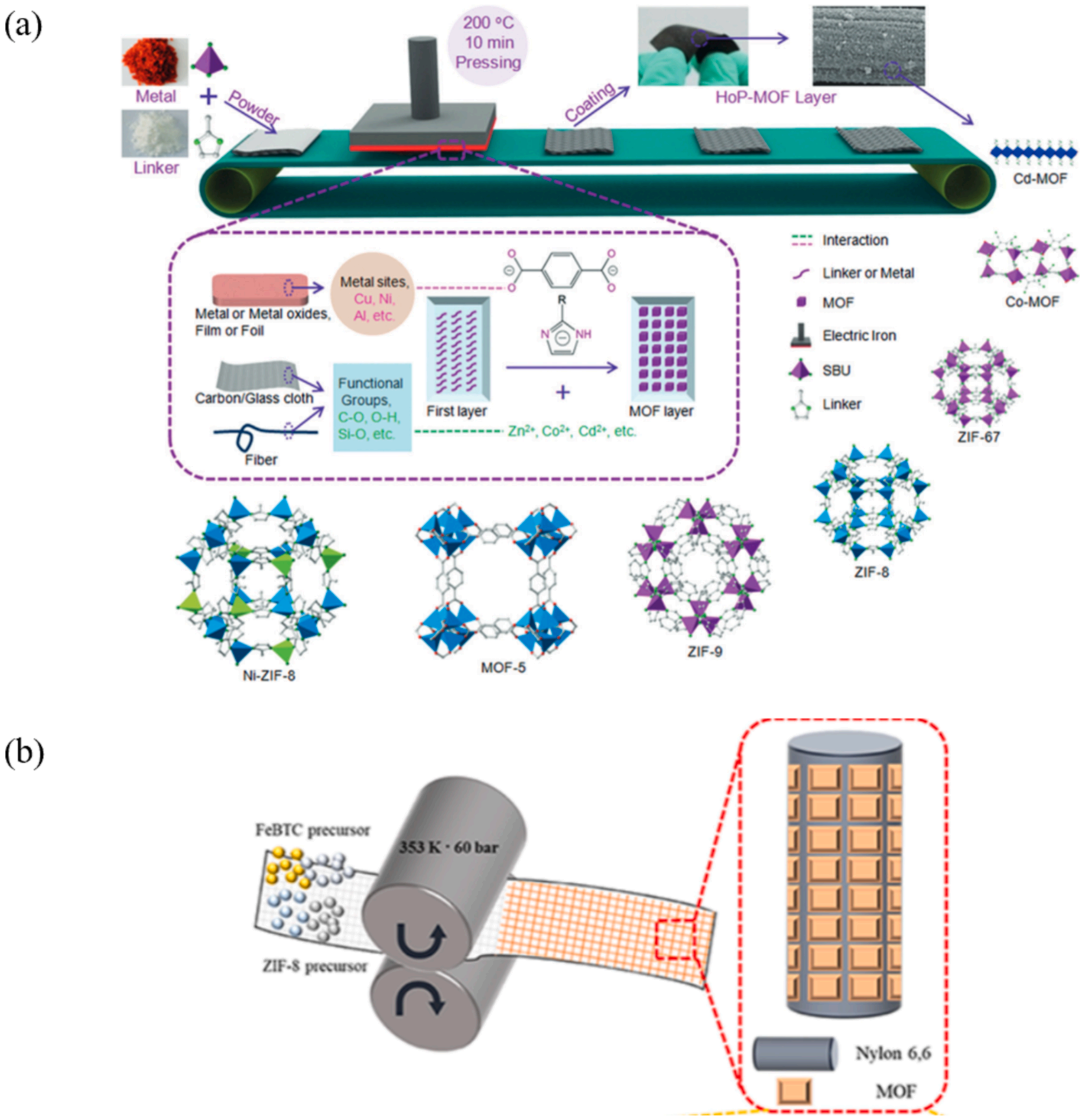

Fig. 5. (a) Schematic presentation of HoP method for MOF coating[83]; (b) Schematic presentation of roll-to-roll method for MOF coating[209].

the membrane, a hair straightener was used to keep the upper surface and undersurface heated simultaneously during the fabrication of MOFs-coupled-fiber membranes by the HoP method [85]. The well-developed membranes could be achieved under a relatively low temperature (80 °C) and a short time (5 min). Also, the distribution of MOF crystals showed a clear trend from sparse to dense with the increase of HoP cycles.

Though the HoP method is efficient for the development of a series of MOFs-coupled-fiber membranes, it is non-applicable to high-valence-metal-based MOFs (e.g., Zr-MOFs). To realize the embedding of those MOFs on the substrate by the HoP method, deep eutectic solvent (DES), which is composed of hydrogen bond acceptor and hydrogen bond donor, can be applied to significantly promote the contact of MOF precursors and accelerate the formation of Zr-MOFs [81]. Following this strategy, choline chloride (ChCl) and urea were chosen as hydrogen bond acceptor and hydrogen bond donor respectively, and different types of Zr-MOFs (UiO-66, UiO-66-NH_2, UiO-66-$(OH)_2$, UiO-66-Br_2 and MOF-801) were fabricated on nonwoven fabrics via HoP processes. The morphology of MOF crystals could be controlled by altering the dosage of DES and modulator (acetic acid), the reaction temperature, as well as the reaction time. Overall, the DES-assisted HoP method is considered a facile way to prepare Zr-MOFs-coupled-fiber membranes.

2.2.2. *Layer-by-layer growth*

Layer-by-layer (LbL) growth is an efficient approach for promoting MOF growth on fiber substrates, which is similar to the direct solvothermal growth strategy [28,86]. However, the LbL approach could be performed at ambient conditions without the need for high reaction temperature and pressure. Furthermore, the functionalized fibers could result in a uniform dispersion of MOF particles on the fiber substrate with multiple repetitions of alternate immersion into metal ion solution and ligand solution [87]. It is noteworthy that the hinge of the LbL strategy is the pretreatment of substrates, which binds between substrate fibers and metal ion precursors of MOFs. For example, treating electrospun carbon nanofibers with ozone could generate abundant negatively charged surface functional groups (e.g., carboxyl), serving as active sites for the nucleation of ZIF-8 [88]. The synthesis was accomplished by dipping the carbon nanofiber membrane in Zn^{2+} solution and 2-MI solution alternately. Due to the electrostatic force, Zn^{2+} was absorbed by negatively charged carbon nanofibers, and 2-MI reacted with the absorbed metal ions to form well-adhered ZIF-8 subsequently.

Natural fibers, which are rich in functional sites (e.g., carboxylates, amines, etc.), are ideal substrates for LbL synthesis[72]. Cotton fibers could be treated with NaOH for deprotonation of hydroxyl groups, then applied to LbL-fabricated zinc 1,4-benzenedicarboxylate (ZnBDC)-cotton fibers [87]. The MOFs loading amount, the thickness of the MOF layer, and the dispersion of MOFs could be altered by modulating the LbL cycles as shown in Fig. 6**a-c**. However, for stable immobilization of MOFs, chemical bindings are essential [89]. Therefore, more complex modifications and the introduction of functional groups could be involved. For instance, lignocellulosic fiber was carboxymethylated to bind Cu^{2+}, further hybridizing with HKUST-1 as shown in Fig. 6**d** [90].

To promote the crystallization of MOFs on the fiber, ultrasound could be introduced during the LbL strategy. Morsali *et al.* [91,92] investigated an ultrasound treatment-assisted LbL method to grow HKUST-1 and MOF-5 on silk fiber membranes. After treating with the alkaline solution for deprotonation, the substrate was subsequently dipped into a solution composed of metal salts and organic ligands under ultrasonic irradiation for the crystallization of MOFs. Different from those without ultrasonic assistance, MOFs formed by this strategy presented cubic morphology as well as homogeneous distribution.

2.2.3. *Atomic-layer-deposition-assisted growth*

Atomic-layer-deposition (ALD)-assisted growth strategy is a facile route to assemble MOFs on fiber membranes. Nanofibers are precoated with metal oxides (e.g., Al_2O_3, TiO_2, ZnO, etc.) via atomic layer deposition , then the development of MOF particles occurs on the surface of ALD layers. A cycle of ALD is composed of two half-reactions as shown in Fig. 7**a**. The first step is to add a metal-containing precursor of metal oxide layers, which reacts with hydroxyls on the surface of substrates. Another precursor containing oxygen (e.g., deionized water) is further dosed to form the metal oxide layer. The two steps can be repeated until the satisfactory metal oxide layer is obtained [71,93]. ALD coatings of metal oxide layers could increase the surface roughness and change the wettability of fibers, facilitating the permeation of solvothermal solvents, consequent in the improvement of reactivity and nucleation between MOF precursors and fiber substrate, resulting in a higher loading amount and more homogeneous dispersion of MOFs on the fiber substrates[94]. ALD-assisted growth is especially a suitable approach for those fibers that are difficult to load MOF particles directly.

Zhao *et al.* [19] demonstrated the ALD-assisted route for growing MOFs on fiber membranes, which achieved high MOF loading, large specific surface areas, and applicability to a variety of substrates (e.g., Polypropylene (PP), polybutylene terephthalate (PBT), cotton, etc.) and MOFs (e.g., HKUST-1, MOF-74, UiO-66, etc.). Take HKUST-1/PP fiber membranes for example, Al_2O_3 layers were coated on the surface of PP

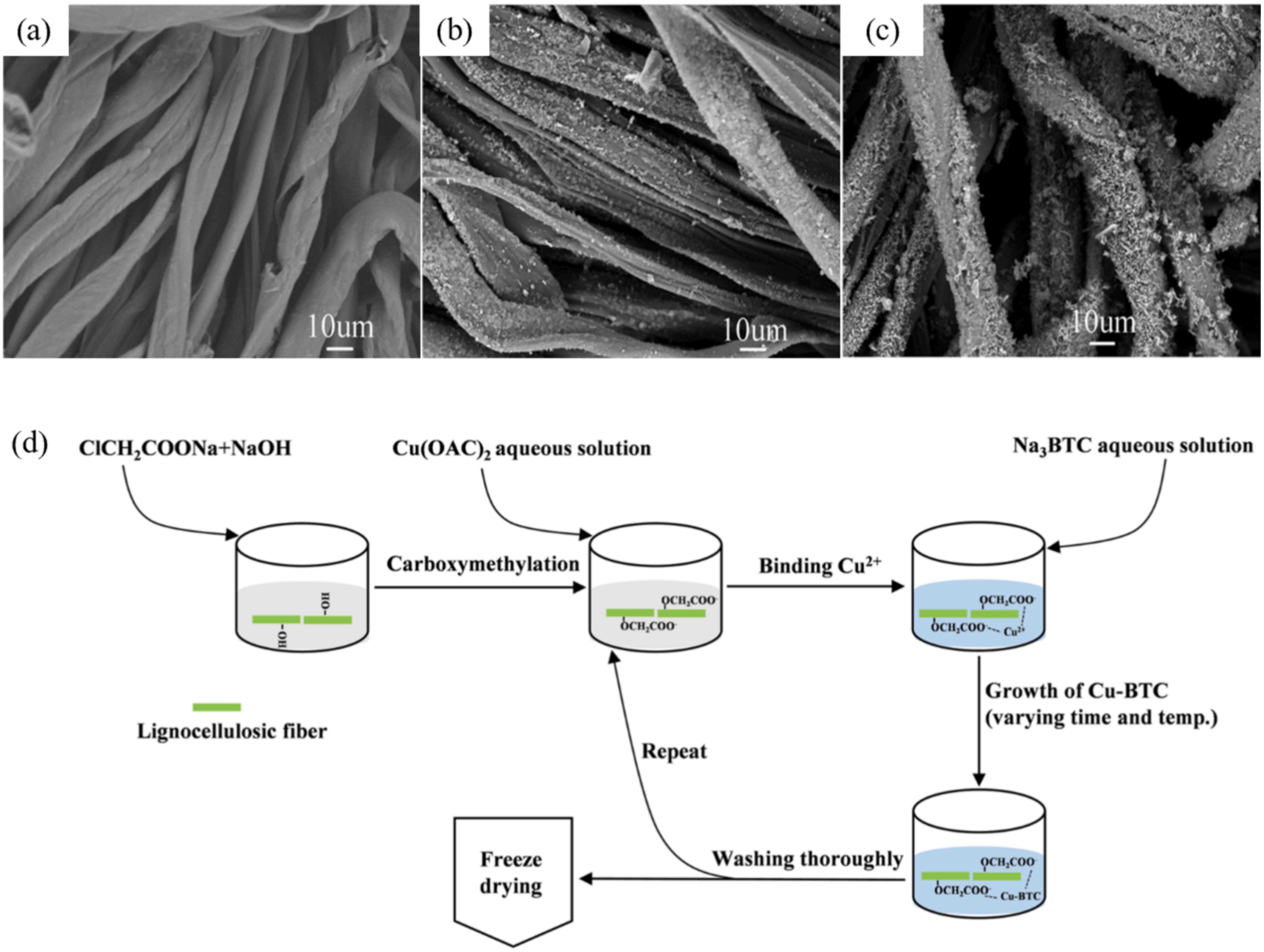

Fig. 6. SEM images of (a) pristine cotton fabric, (b) ZnBDC-fiber of 3 LbL cycles, (c) ZnBDC-fiber of 8 LbL cycles[87]; (d) Schematic of the preparation of HKUST-1@CHFs[90].

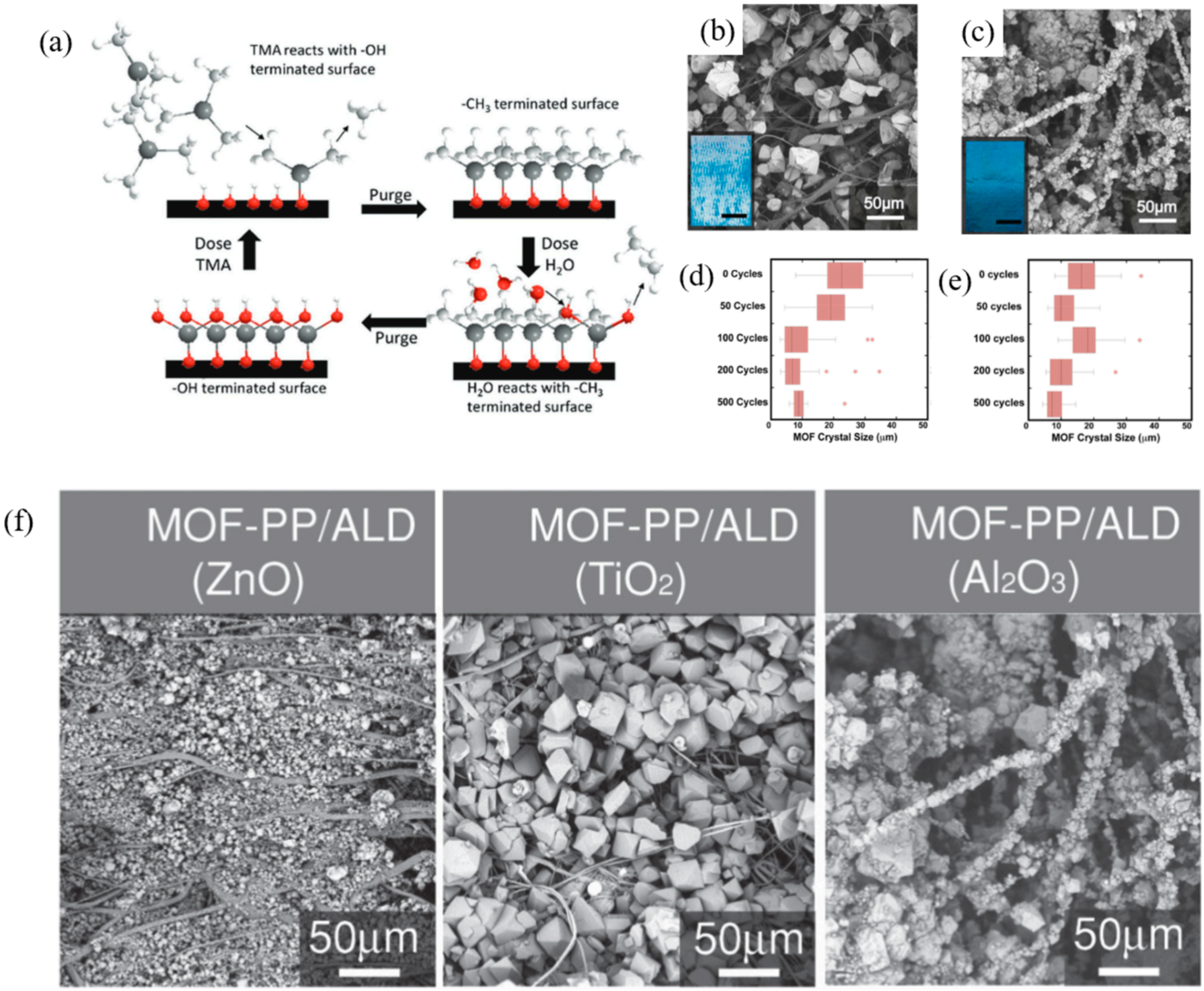

Fig. 7. (a) Schematic illustration of the Al_2O_3 ALD process[93]; SEM image of (b) HKUST-1 MOF grown on untreated polypropylene fiber mats (MOF-PP), (c) SEM image of HKUST-1 MOF grown on ALD-Al_2O_3-coated polypropylene fiber mats (MOF-PP/ALD)[19]; MOF-fiber mats with different ALD coating thicknesses: (d) MOF crystal size distribution on the top surface, (e) MOF crystal size distribution on the cross-section[19]; (f) HKUST-1 MOF grown on different ALD coatings[19].

fibers first, and then HKUST-1 was grown on the surface of PP-Al_2O_3. As shown in Fig. 7**b, c**, the ALD-assisted PP fibers showed more uniform MOF coverage compared with untreated PP fibers, indicating heterogeneous nucleation on the fiber surface. The specific surface area of ALD-assisted MOF-PP was 60 % higher than that of MOF-PP fibers as well. Furthermore, a systematical change in the thickness of ALD layers could also control the distribution of MOF crystal size. As shown in Fig. 7**d, e**, with the increase of ALD cycles, the average size of MOF crystals decreased and the size distribution scope narrowed. Different metal oxide coatings could also affect the nucleation of MOF crystals, consequently affecting the morphology of MOF-based fibers for the discrepancy of wettability, surface roughness, and isoelectric points of metal oxides (Fig. 7**f**).

2.3. *Coupling pre-synthesized MOFs with fibers*

Fabricating MOFs-coupled-fiber membranes from pre-synthesized MOFs is another feasible option, during which MOFs are produced precedingly. The valid connection between MOFs and fiber substrates is essential to avoid the aggregation and run-off of MOFs. Doping during electrospinning, and covalent immobilization coating are two main strategies which are discussed in this section.

2.3.1. *Doping during electrospinning*

Doping MOFs during the electrospinning process is an ideal route for the development of MOFs-coupled-fiber membranes. The direct electrospinning method mainly consists of three steps, 1) pre-synthesization of MOF particles, 2) preparation of MOF-polymer electrospun precursor solution, and 3) direct electrospinning of the precursor solution. For example, Wang *et al.* [95] reported the ZIF-67 nanoparticles immobilized on electrospun PAN nanofibers. Pre-synthesized ZIF-67 particles were dispersed in the DMF solution, and then PAN was added in and stirred to form a homogeneous electrospun precursor solution. After electrospinning, uniform ZIF-67/PAN nanofibers were obtained. Compared with pristine PAN fibers, the surface of ZIF-67/PAN nanofibers was no longer smooth, and the cubic ZIF-67 nanoparticles could be observed in enlarged SEM and TEM images, which can be seen in Fig. 8.

Doping MOFs during electrospinning is a universal technique for a variety of MOFs and polymer substrates, during which the fiber morphology and loading amount of MOFs could be altered. However, one drawback of this strategy is that MOF particles are prone to

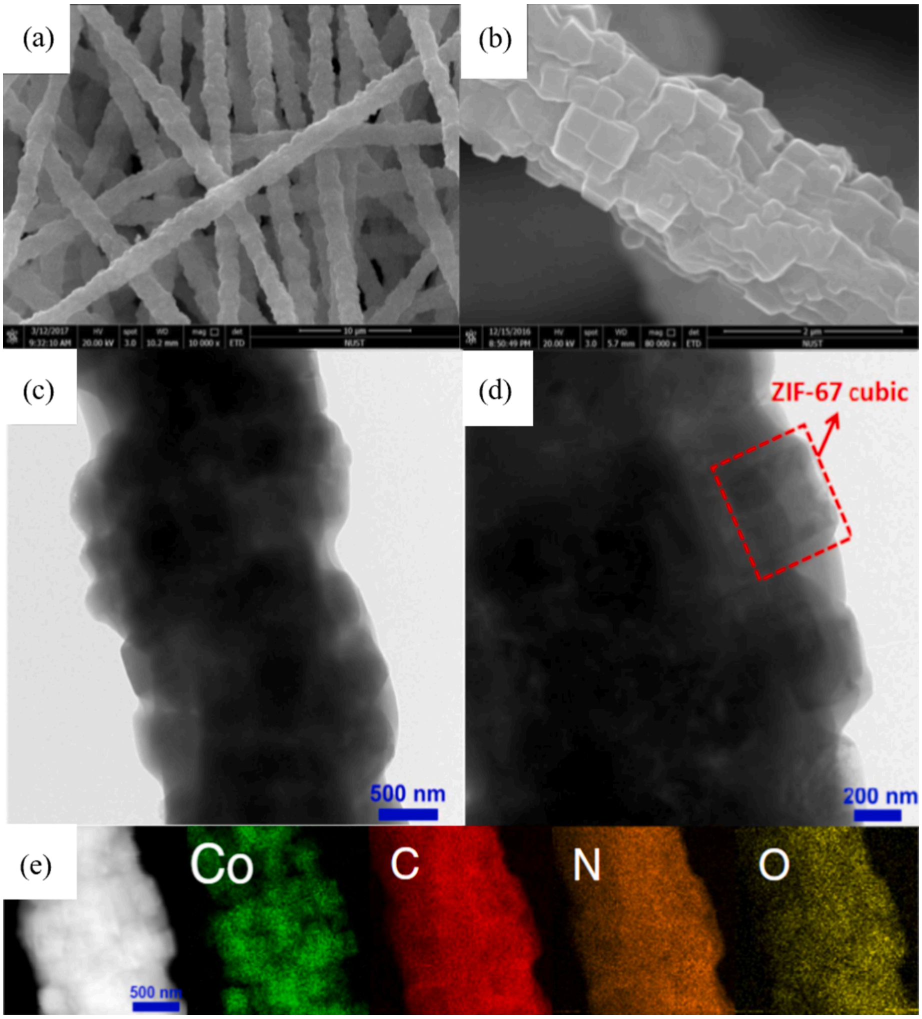

Fig. 8. (a, b) SEM images, (c, d) TEM images of ZIF-67@PAN; (e) STEM image and the corresponding mapping of ZIF-67@PAN[95].

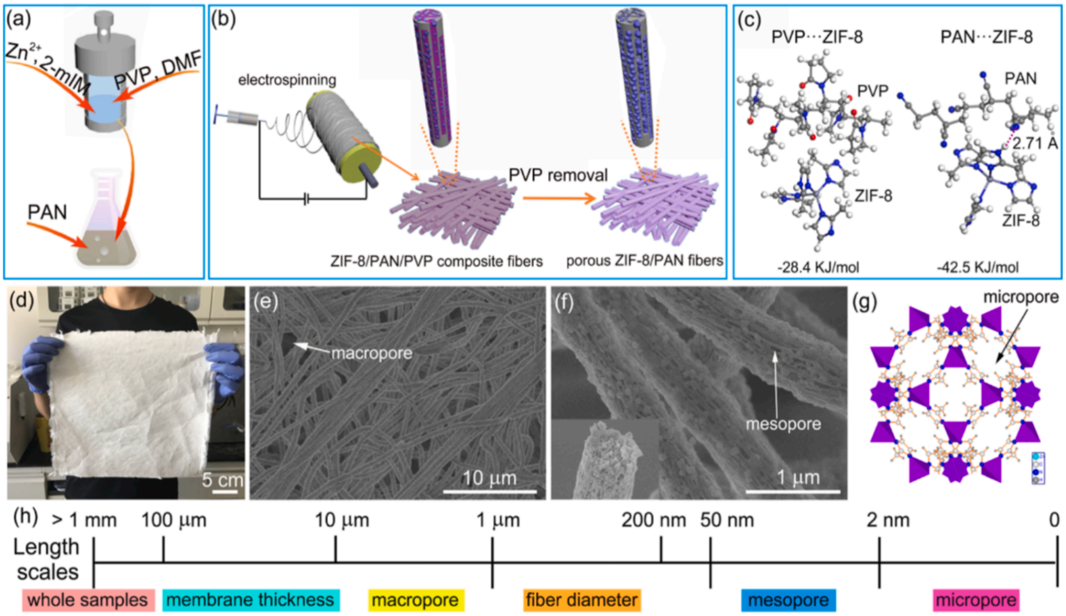

Fig. 9. Schematic illustration of (a) electrospinning solution preparation and (b) fiber preparation; (c) optimized geometries for the configuration of PVP and PAN with the ZIF-8/PAN nanofibers; (d) optical images of porous ZIF-8/PAN fibers; (e, f) SEM images of porous ZIF-8/PAN nanofibers; (g) structure of ZIF-8; (h) the levels of hierarchical scales[98].

agglomeration during the blending process, resulting in uneven distribution of MOF on the fibers. To avert the agglomeration of MOF particles, a small portion of the polymer was firstly added to the MOF suspension, and then the rest of the polymer could be added. For example, Zhang *et al.* [96] achieved the uniform distribution of different MOFs on the electrospun nanofiber. By adjusting the electrospinning parameters (e.g., applied electric voltage, flow rate of the solution, etc.) and the concentration of both PAN and MOFs, MOF nanoparticles were well dispersed even at the loading amount of up to 60 % and the diameters of the fibers could be altered from 200 nm to 1 μm [96]. In another interesting work, An *et al.* [97] introduced polymers into the precursor of ZIF-7, and then heated to crystalize ZIF-7. Accordingly, ZIF-7 nanoparticles were homogeneously distributed in the electrospun polymeric fiber.

In addition to the complicated fabrication process, there is another deficiency of this strategy. During the formation process of MOF-based fiber, MOF particles not only exist on the surface of the fiber, but also be buried inside the fiber, which could impede the contact between MOFs and the pollutants. To expose more available MOF particles, constructing interconnected mesopores in the MOFs-coupled-fibers is an advanced route for enhancing the utilization of MOFs [98]. For example, PVP could be introduced into the fabrication of PAN/ZIF-8 fibrous membrane, which is regarded as a sacrificial pore-forming agent. After immersion in an ethanol solution, PVP was dissolved, which obtained the mesoporous channels inside the fiber as shown in Fig. 9. The macropores provided more adsorption space and reduced the mass transfer resistance, the interconnected mesoporous channels were beneficial to the diffusion of pollutant molecules to MOFs, and the micropores in ZIF-8 could improve the specific area and provide more connection sites of composite fiber membrane.

2.3.2. *Covalent immobilization coating*

The covalent combination of pre-synthesized MOF particles and pre-synthesized fiber substrates is efficient for large-scale applications [82]. The polymer substrates are usually treated beforehand to introduce desired functional groups, facilitating the covalent linking with MOFs. For example, a covalent synthesis method was developed to embed MOFs onto polyester/cotton (PETco) textile fibers [99]. The cotton fraction in PETco fibers was pretreated for carboxylation as shown in Fig. 10**a**. After reacting with NaOH, PETco-COOH fibers further covalently combined with MOF-199 and UiO-66-NH$_2$ to compose the hybrid fiber (Fig. 10**b**).

Initiated by γ-ray irradiation, covalent immobilization of MOFs and the fiber substrate by co-graft polymerization can be achieved. For example, the pre-synthesized MIL-101 particles were added into monomer solutions containing HEA to prepare the suspension. The surface of the nylon fabric was coated with the suspension and irradiated by a Co^{60} γ-ray source at room temperature to initiate the covalent reaction. The generation of free radicals on MIL-101(Cr) under γ-ray irradiation was the key to the linking between MIL-101(Cr) and nylon fabric, initiating the graft of polymerization of HEA on MIL-101(Cr). The co-graft polymerization generated a three-dimensional network that firmly immobilized the MIL-101(Cr) particles (Fig. 10**c**) [100].

A covalent immobilization strategy could combine with ALD-assisted growth to improve the loading efficiency of MOFs. Lee *et al.* [101] fabricated UiO-66-NH$_2$/PP fibers using a self-assembly method combined with ALD synthesis. ALD method was used to create metal oxide layers (Al$_2$O$_3$, TiO$_2$, and ZnO) on PP fibers, and the self-assembly agent replenished the hydroxyl groups on the surface of PP fibers, which was essential for covalent bonds between MOFs and substrates. Compared with PP/MOF fibers, PP-metal oxides/MOF fibers demonstrated a higher loading amount and more uniform dispersion of MOFs on fibers. The self-assembly agent promoted the adhesion of MOFs and made a difference in minimizing MOF crystal aggregation in the mixed suspension, further resulting in even distribution over the entire membrane.

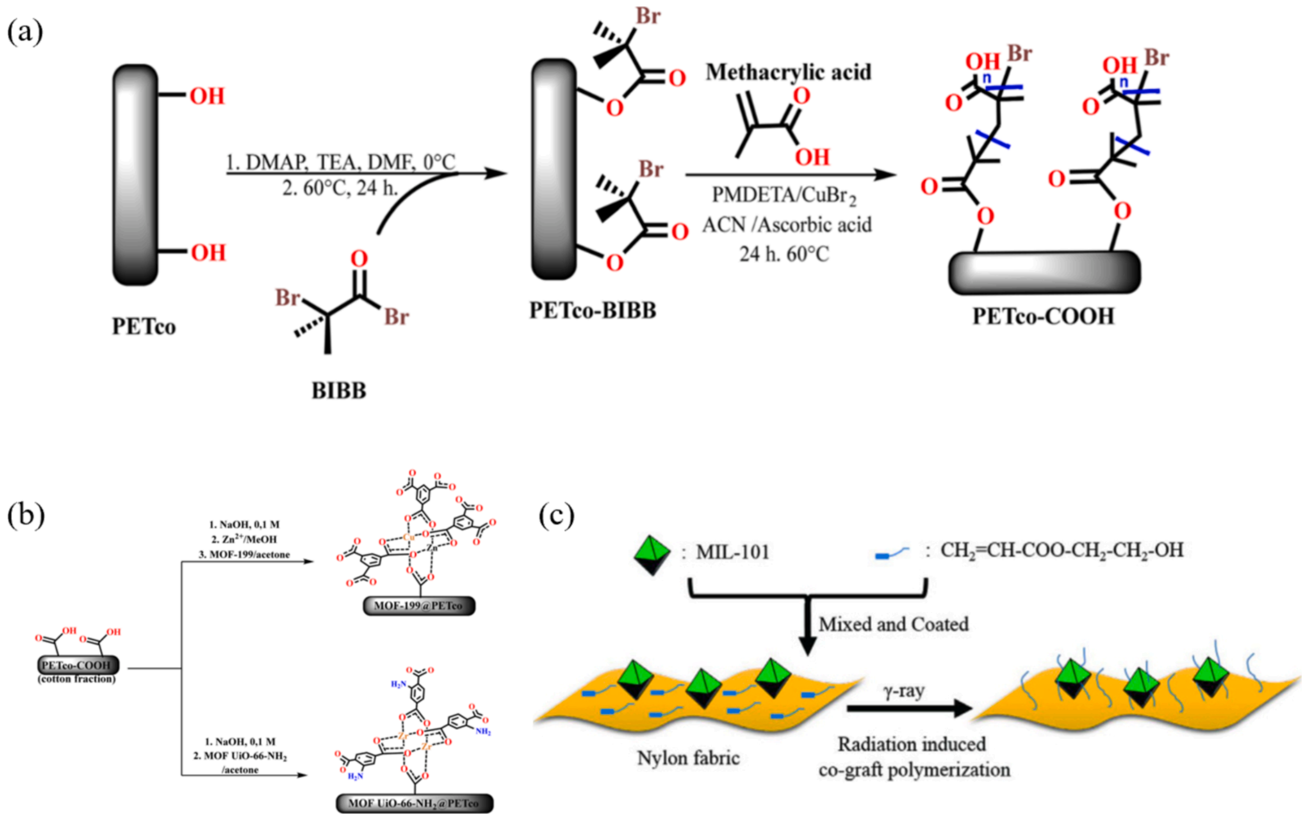

Fig. 10. (a) Synthetic pathway for the ATRP-ARGET carboxylation of the cotton fraction in PETco fibers; (b) Procedures of covalent immobilization of MOF-199 and UiO-66-NH$_2$ on PETco[99]; (c) Preparation of nylon fabrics immobilized with MOFs by radiation-induced graft polymerization[100].

2.4. Pros and cons of different preparation strategies

Conventional solvothermal synthesis enables uniform coatings of MOFs on the fiber surface. In detail, direct solvothermal growth is one of the commonly used methods, which achieves well-attached growth of MOFs to various fiber-based substrates. For the inert substrates, modification with functional groups to facilitate the growth of MOFs is advisable. However, due to there being no anchor seeds inside substrate fibers, the nucleation of MOFs mainly occurs in the solvent, resulting in reduced amount of MOF growth on the fiber. Compared with direct solvothermal growth, seed-assisted secondary growth could develop MOFs-coupled-fiber membranes with a higher MOF loading amount. Despite this approach could only be achieved by electrospinning, the morphology and structure could be modulated by altering the ratio of seeds and polymers as well as the parameters during electrospinning. Besides, MOF particles are half-inserted in fibers, which ensures a tight combination between fibers and MOFs.

The operation process of HoP method is simplified to a certain extent since the solvents are not involved. The HoP method is suitable for a series of MOFs and substrates, and the roll-to-roll method based on this strategy could achieve mass production [80]. By adjusting the number of coating layers, different loading amounts of MOFs could be achieved. Noticeably, this strategy is not feasible for MOFs and substrates with poor thermal stability. The advantage of layer-by-layer growth is that it can occur under mild conditions. The alternate dipping of the substrates into metal ions and organic ligand precursors yields a homogeneous dispersion of MOFs. The nucleation of MOFs can be promoted by the functional groups on substrates, e.g., carboxyl, amino, etc. Additionally, the loading amount is improved and the particle size of MOFs is enlarged with the repetition of LbL cycles. Notwithstanding, the functionalization of fiber substrates with specific functional group modifications requires a relatively cumbersome synthesis process. The ALD-assisted method provides a pathway for the combination of MOFs and fiber substrates, especially for the fibers that were originally difficult to combine with MOFs.

Due to the independence of MOF synthesis and fiber formation processes, fabricating MOFs-coupled-fiber membranes from pre-synthesized MOFs is relatively easy to operate. Therefore, doping during electrospinning can be applied to a wide range of MOFs, during which the MOF loading amount, the morphology and structure of fibers could be alterable by adjusting the electrospinning parameters. Also, the nucleation of performed MOF particles could lead to high-quality crystals. While the drawback is that part of MOF particles is encapsulated inside the fiber, decreasing the utilization efficiency of MOFs. The covalent immobilization method is applicable to commercial substrates. Compared with doping during the electrospinning method, MOF particles scatter evenly on the fiber surface, preserving the intrinsic properties of MOFs to a large extent. Nevertheless, the required additives of covalent bonding make the developing process relatively intricate.

3. Applications of MOFs-coupled-fiber membranes in removing contaminants from water

In recent years, MOFs have been considered as a kind of ideal material for water purification because of their crystalline nature, high specific surface area, tunable functionalities, and plentiful species [102,103]. The crystalline nature and high specific area facilitate the adsorption of pollutants [104]. The tunable functionalities and plentiful species of MOFs bring them adequate selectivity for numerous contaminants as well as coping strategies for complex contaminants [105,106]. However, MOF particles may detach from the fiber and enter into the water environment when they are not firmly bonded to the substrate [107]. Encrusting MOFs into flexible fibers could improve mechanical stability, reusability, and durability in aqueous conditions [103]. Moreover, with a proper combination of high surface-to-volume ratio fibers, the increased active surface of MOFs in contact with the environment could further enhance the probability of trapping the pollutants [46]. Due to the large specific surface area of the flexible fiber, there will be an enhanced MOF loading. The increased active surface of MOFs in contact with the environment could further enhance the probability of controlling the pollutant. Here, we discuss the purification performance of MOFs-coupled-fiber membranes for several contaminants, such as heavy metal ions, organic dyes, and emerging pollutants. The structure, development methodologies, of MOFs-coupled-fiber membranes, and related effects on purification performance for each typical pollutant are systematically analyzed.

3.1. Heavy metal ions

Heavy metal pollution has been regarded as a global environmental threat and extensively studied by researchers, including cadmium (Cd), arsenic (As), lead (Pb), chromium (Cr), mercury (Hg), silver (Ag), etc., which are nonbiodegradable and tend to bioaccumulate as the food chain prolongs [108,109]. Though trace amounts of heavy metal elements are essential for human health, excess amounts could result in serious health problems [110–116]. Therefore, finding efficient and scalable approaches is crucial for removing heavy metals from aqueous solutions. Traditional ways of heavy metal removal face several challenges that to be overcome, e.g., lack of selectivity, secondary pollution, low efficiency, low reusability, etc. [117]. MOFs-coupled-fiber membranes have attracted incredible attention to satisfy these challenges. Heavy metal removal based on membrane purification can be categorized into three mechanisms, such as membrane filtration, adsorption, and catalytic reduction [118–120]. Membrane filtration is the predominant mechanism for membranes with pores smaller than heavy metal ions, while for membranes with pores larger than heavy metal ions, the purification process could be controlled by adsorption [71]. Catalytic reduction is used to detoxicate multivalent heavy metals, during which MOFs-coupled-fiber membranes act as heterogeneous catalysts.

Among heavy metals, As is found to pose the most adverse effects on human health, which can cause abnormalities in RNA (ribonucleic acid) and DNA (deoxyribonucleic acid) by replacing phosphate, eventually leading to the developing cancers in the lungs, kidneys, bladder, and skin [121–127]. As exists in aqueous solutions in both inorganic and organic forms. The inorganic type of arsenic is highly toxic and usually in the states of arsenite (As (III)) and arsenate (As (V)), while its organic type is less hazardous. For efficient removal of As (III) and As (V), the UiO-66/PAN composite was prepared by doping during the electrospinning method [128]. The prepared UiO-66/PAN nanofibers (Fig. 11**a**) possessed As (III) and As (V) adsorption capacities of 32.90 mg/g and 42.17 mg/g respectively. Compared with the adsorption capacities of pure UiO-66 samples, however, the maximum adsorption capacity decreased a lot (from 127 and 212 mg/g to 32.90 and 42.17 mg/g, corresponding to As (III) and As (V) respectively). The difference in adsorption performance could be ascribed that most of the UiO-66 particles were enclosed by PAN in fibers. To expose more MOF particles to the environment, Kong et al. [129] introduced graphene oxide (GO) to the electrospun precursor for As (V) adsorption. As shown in Fig. 11**b**, the as-prepared MOF-808/PVDF/GO fiber membranes provided adequate pores for connection and mass transfer between MOF particles and arsenate ions. The introduction of GO particles into PVDF nanofibers had a significant impact on the formation of porous fibrous structures. The strong repulsive force between GO particles under high voltage during electrospinning causes the stretching and cracking of the surrounding polymers, leading to the generation of numerous nanopores. The maximum adsorption capacity was over 180 mg/g (Fig. 11**c, d**), and over 80 % of the initial adsorption efficiency remained after four cumulative recycle tests. The superior adsorption performance was mainly attributed to the coordination and π-π reaction between MOF-808 and As ions. Pang and co-workers [130] prepared MIL-88A (Fe) on the surface of cotton fibers using covalent immobilization coating

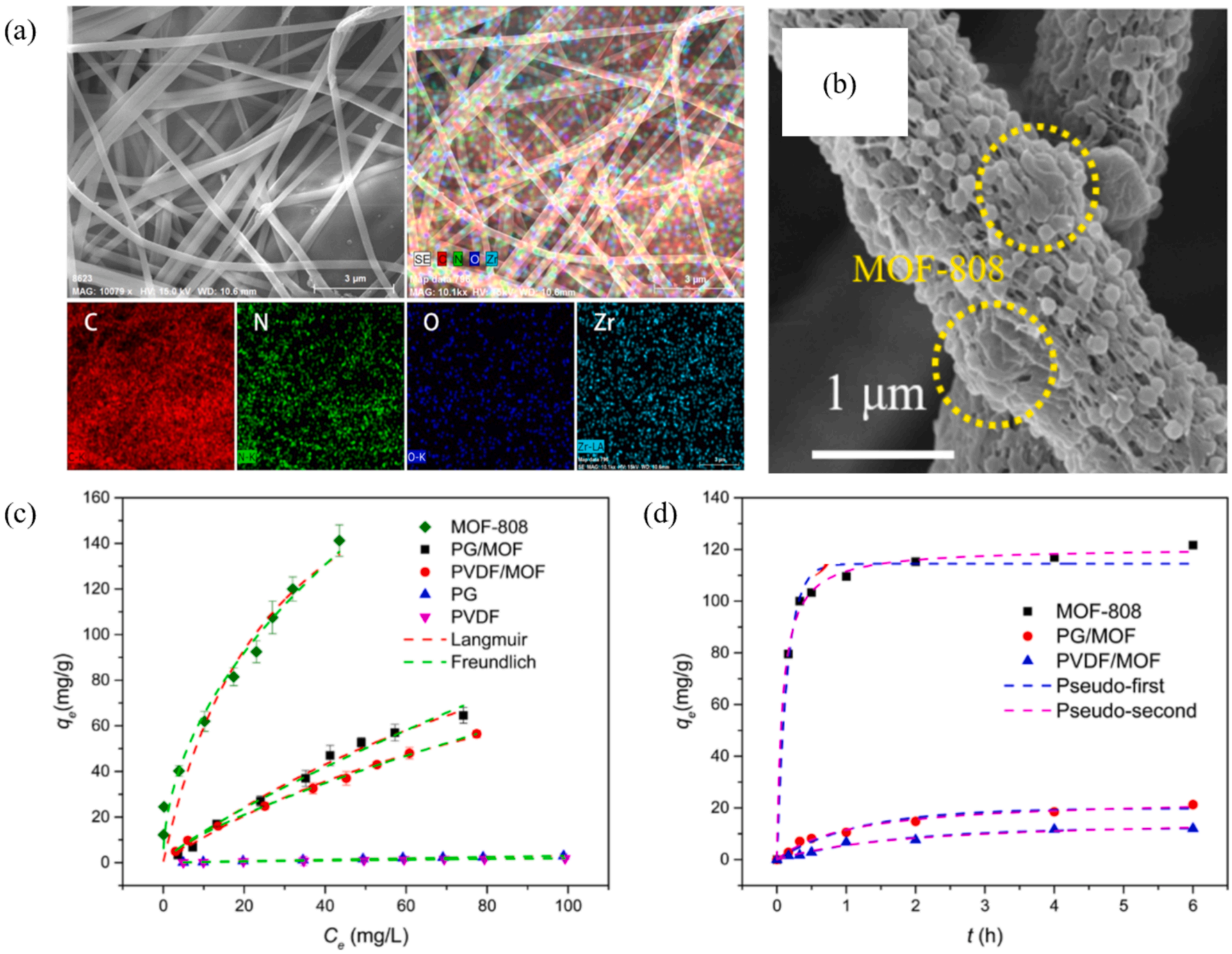

Fig. 11. (a) SEM and elemental mapping of the as-prepared 10 wt% UiO-66/PAN nanofiber[128]; (b) SEM images of electrospun PG/MOF nanofibers[129]; arsenate adsorption (c) isotherms and (d) kinetics for MOF-808, PG/MOF, PVDF/MOF, PG and PVDF[129].

and direct solvothermal growth method, respectively, which enabled more MOF particles attached to the fiber surface for further improving adsorption capacity. The proposed MIL-88A (Fe) fiber membranes exhibited superior adsorption performance for arsenic pollutants, even almost the same as the original MIL-88A (Fe) particles. Moreover, the leakage of iron of the composite membrane is much lower than that of the original MIL-88A (Fe), which also reflects the superiority of the membrane.

Cr exists in both trivalent Cr (III) and hexavalent Cr (VI) within the aqueous solutions. Cr (VI) with higher biological toxicity could cause cancer diseases in the digestive system and lungs as well as other severe health hazards (e.g., skin dermatitis, bronchitis, diarrhea, etc.) [131–137]. To control Cr (VI) in drinking water, direct adsorption or reducing Cr (VI) to harmless Cr (III) ions have been regarded as the main effective techniques. The Fe-MOF/PAN electrospun fiber membranes synthesized through doping during the electrospinning technique were proposed for the removal of Cr (VI) from water [138]. Although Fe-MOF/PAN fibers exhibited the porous structure, the encapsulated MOF particles inside the fiber hindered the adsorption capacity. The adsorption capacity of Fe-MOF/PAN fibers was 127.70 mg/g, while that of the pristine Fe-MOFs was 229.42 mg/g. The mechanisms of adsorption of Cr (VI) included electrostatic interaction, redox reaction, coprecipitation, coordination effect, etc. (Fig. 12**a**). Moreover, part of Cr (VI) was captured by Fe-MOF and reduced to Cr (III) with the reducibility of –OH groups and Fe (II) ions from Fe-MOFs. However, the adsorption of Fe-MOF/PAN fibers was dominated by physical adsorption, in which the removal efficiency was limited. To accomplish the highly efficient selective adsorption and catalytic reduction performance of Cr (VI), a nylon-6@UiO-66-NH_2 electrospun fiber membrane was synthesized through seed-assisted secondary growth, with the surface area reaching 287 m^2/g [139]. The partially-embedded nature of UiO-66-NH_2 nanoparticles surrounding the fibers could provide more adsorptive sites (Fig. 12**b, c**). Apart from physical electrostatic interaction, the nitrogen-containing functional groups from UiO-66-NH_2 played an important role in chelation reactions with Cr (VI), improving the adsorption capacity to 202.79 mg/g as shown in Fig. 12**d**. Furthermore, due to the support of nylon-6 fibers which avoided aggregation of MOFs and therefore enhanced the light absorption, the photocatalytic capacity of nylon-6@UiO-66-NH_2 fiber membrane for Cr (VI) was 27.1 mg/g, almost twice that of pure UiO-66-NH_2 powder (15.5 mg/g). After recycling 5 times, over 80 % of the reduction efficiency still existed, showing high recovery and regeneration properties in water purification.

Pb is classified as a persistent environment toxic substance which may cause mental disturbance, retardation, and semi-permanent brain damage[140–147]. Currently, MOF-based adsorbent materials, particularly nanofiber composites, have become one of the popular candidates for removing Pb ions from water. Shooto *et al.* [148] fabricated a series of MOF-based fiber composites (Sr-TBC/PVA, La-TBC/PVA, and Sb-TBC/PVA, where TBC referred to benzene 1,2,4,5-tetracarboxylate adsorbents) to remove Pb (II) ions from aqueous solutions by doping during electrospinning method. Accordingly, the maximum adsorption capacities of 91, 124, and 194 mg/g were measured for Sb-TBC/PVA, Sr-TBC/PVA, and La-TBC/PVA nanofiber composites, since the mechanism of La-TBC/PVA and Sr-TBC/PVA were predominated by chemical adsorption while the adsorption by Sb-TBC/PVA was mainly physical

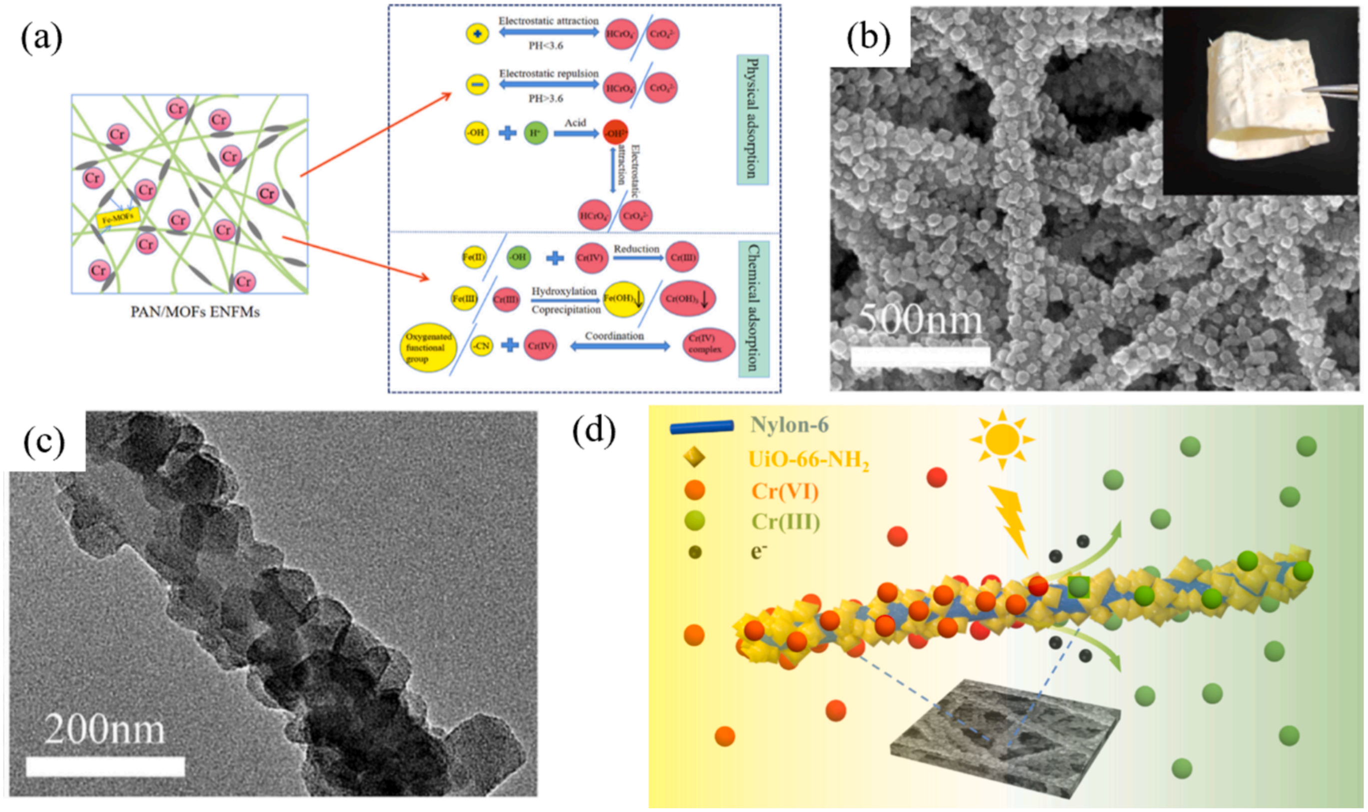

Fig. 12. (a) Adsorption mechanism diagram of PAN/MOF ENFMs for Cr(VI) in water[138]. (b) SEM and (c) TEM images of nylon-6@UiO-66-NH_2[137]. (d) Schematic diagram of preparation of nylon-66-NH_2 fiber membrane[137].

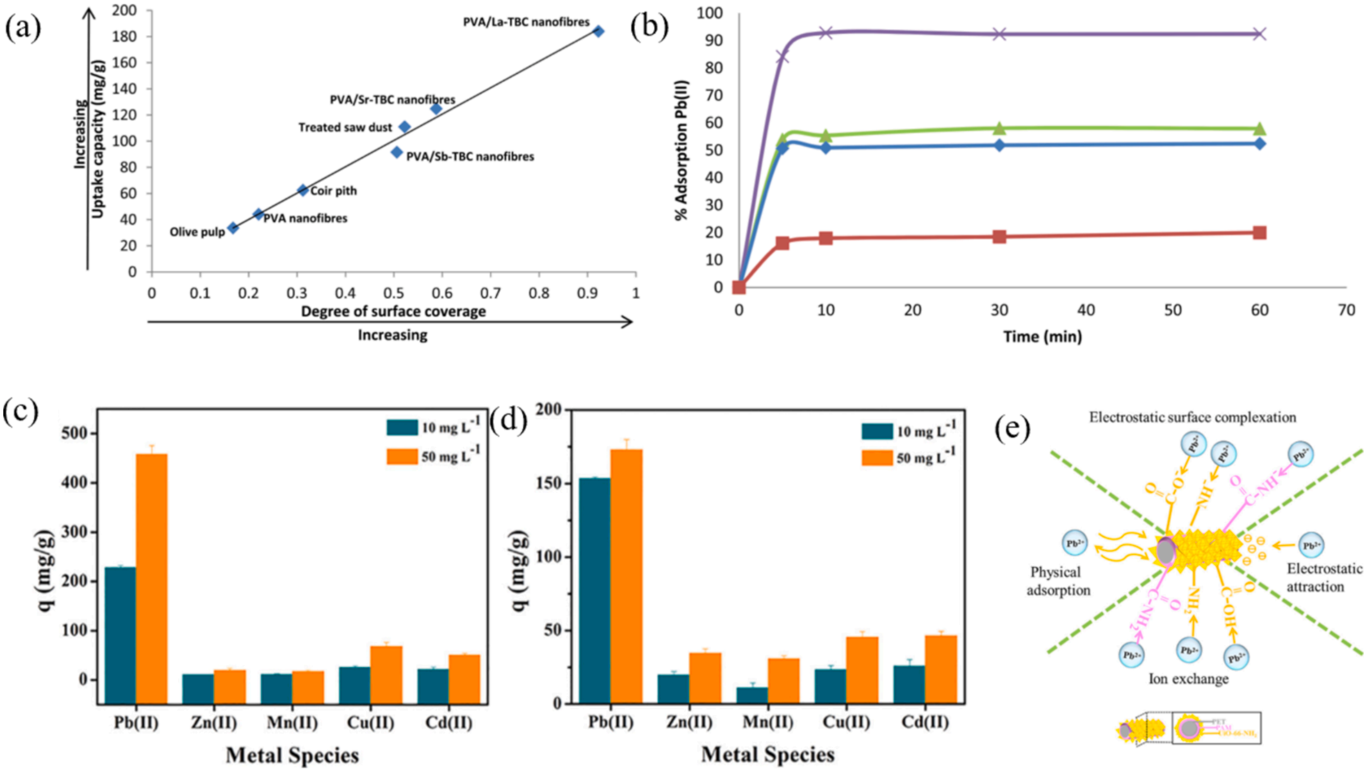

Fig. 13. (a) Maximum adsorption capacity of nanofibers against some activated carbons[148]; (b) Time dependence studies on the sorption of Pb (II) ions onto PVA nanofibers (filled square), PVA/Sb-TBC nanofibers (filled diamond), PVA/Sr-TBC nanofibers (filled triangle) and PVA/La-TBC nanofibers (X mark)[148]; Selective adsorption of UiO-66-NH_2-PAM-PET toward five single (c)and mixed (d) ions[149]; (e) Proposed Pb(II) adsorption mechanism on UiO-66-NH_2-PAM-PET[149].

adsorption. It was also observed that the adsorption capacity improved with the increasing surface coverage of MOFs on the fiber (Fig. 13**a**), which could be attributed to the more adsorptive sites and a larger surface area of the composite membrane. Moreover, the adsorption process of Pb (II) was rapid (reached adsorption equilibrium at about 5 min as shown in Fig. 13**b**). The increased Pd adsorption capacity of MOFs-coupled-fiber membranes could also be achieved using a direct solvothermal growth strategy [149]. The polyethylene terephthalate (PET) nonwoven fabric was modified by polyacrylamide (PAM) to facilitate the nucleation of UiO-66-NH_2 to achieve the UiO-66-NH_2-PAM-PET composite. Benefiting from the intrinsic merit of UiO-66-NH_2 and the support of PAM-PET fibers, the developed composite exhibited an outstanding adsorption capacity of 711.99 mg/g toward Pb (II), which was even higher than pure UiO-66-NH_2. Furthermore, the composite membrane exhibited a higher adsorption selectivity of Pb (II) than that of other heavy metals (e.g., Cu (II), Cd (II), Zn (II), etc.) (Fig. 13**c, d**). The mechanism for excellent adsorption capacity to Pb (II) could be concluded as a combination of physical and chemical adsorption, in which chemical adsorption was the main mechanism as shown in Fig. 13**e**. The specific area, pore structure of the composite membrane, and the electrostatic attraction between the membrane and Pb (II) enabled favorable physical adsorption.

Cu is an essential trace mineral for human health. However, its excessive intake can cause toxicological issues, even death [150–156]. Removing copper ions from wastewater before being discharged into the water steam is crucial. Recently, a growing interest in removing copper ions from water with MOF nanofibers has been attracted by researchers. For instance, ZIF-67-based "pearl-necklace-like" composite membranes prepared by direct solvothermal method on the surface of 1-methylimidazole/cellulose acetate (MIM/CA) electrospun nanofibers were used for the removal of Cu (II) [157]. The surface area of ZIF-67/CA fibers reached 463.1 m^2/g due to the pearl-necklace structure as shown in Fig. 14**a, b**, which performed a high Cu (II) adsorption capacity of 18.9 mg/g. The adsorption mechanisms could be identified as the combined action of both physical and chemical adsorption, including physical adsorption driven by the concentration gradient and electrostatic attraction, the coordination between Cu^{2+} and the pyridine nitrogen from CA substrates, and the ion exchange between Cu^{2+} and the hydroxyl which bonded with uncoordinated Co^{2+} sites on the surface of ZIF-67/CA fibers. ZIF-8 is also regarded as an option for the removal of Cu^{2+}. With the combination of ZIF-8 by a HoP method, the surface of PAN fiber became rough, and the specific surface area of ZIF-8/PAN reached 154 m^2/g [84]. The ZIF-8/PAN nanofibers exhibited excellent performance with fast flux (12000 L/(m^2h)) and high filtration efficiency (97.65 % at maximum) for Cu^{2+} in dynamic adsorption. The capture effect of copper ions was not affected by the coexistence of multiple metal ions like Ni^{2+}, Mg^{2+}, Cr^{3+}, Co^{2+}, etc. (Fig. 14**c-f**) The dominant action for adsorption was the coordination between Cu^{2+} and pyridine nitrogen from PAN and the ion exchange among Cu^{2+} and Zn^{2+} from ZIF-8, explaining both the selectivity and the high-efficient adsorption.

For the removal of heavy metal ions from water, adsorption is the main role played by MOFs-coupled-fiber membranes, accompanied by catalysis attenuation for multivalent metal ions. Therefore, the exposure of MOFs to contaminants is crucial. Doping during the electrospinning method is a fundamental method for building MOFs-coupled-fiber membranes. The removal efficiency of heavy metal ions is relatively low due to the lack of adsorption sites; however, porosity optimization of fibers is significant to disclose more MOFs and improve adsorption efficiency. Other *in situ* synthesis strategies, including direct solvothermal growth, seed-assisted secondary growth, layer-by-layer growth, HoP, and covalent immobilization coating all provide favorable contact sites, which are promising approaches to prepare MOFs-coupled-fiber membranes given the removal of heavy metal ions.

3.2. *Organic dyes*

Due to the carcinogenic and mutagenic characteristics, organic dyes can cause toxic effects on humans, fauna, and flora, which has been considered a serious environmental issue [158–162]. Organic dyes in water can reduce light penetration and influence the photosynthetic activities in aquatic ecosystems, which are bio-accumulative as well [163–166]. There are more than 10,000 types of synthetic organic dyes, including acridine orange, indigo carmine, rhodamine B (RhB), malachite green, methylene blue, etc. [167]. The removal of organic dyes from water is extremely difficult because of the complex molecular structure, high molar mass, and low biodegradation. Adsorption with membranes has been found as one of the most attractive techniques to remove organic dyes for its easy-operating, high efficiency, and economic approach . However, the relatively fixed morphological feathers

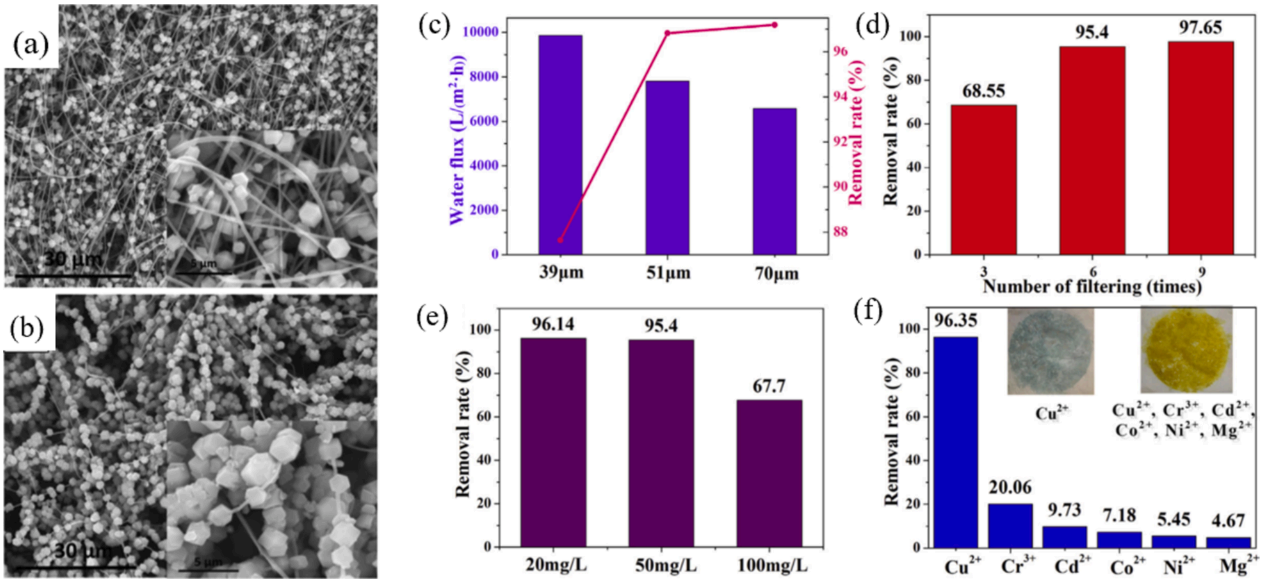

Fig. 14. SEM images of prepared CA/ZIF composite membranes: (a) ZIF/CA-1; (b) ZIF/CA-12[157]; Performance of dynamic filtering heavy metal ion system: (c) water flux and Cu^{2+} removal rate under different membrane thickness; (d) relationship between filtration times and Cu^{2+} removal rate; (e) effect of initial solubility of Cu^{2+} on removal rate; (f) removal efficiency of different heavy metal ions[84].

and insufficient surface area of traditional membrane materials limit their adsorption capacity [91]. Recently, MOFs-coupled-fiber membranes have attracted great interest in removing organic dyes from aqueous systems, which is ascribed to the high porosity, tunable structure, rich functionality, and open metal sites of MOFs.

Adsorption is one of the dominant mechanisms for the removal of organic dyes with MOFs-coupled-fiber membranes. Types of organic dyes that could be adsorbed depend on the electric properties of MOFs-coupled-fiber membranes and organic dyes. For example, bio-MOF-1/PAN fiber membranes were fabricated by doping during the electrospinning method [168]. Owing to the nucleophilic group C≡N of PAN, the proposed MOFs-coupled-fiber membrane could achieve high adsorption of cationic dyes, while negligible removal of anionic dyes. ZIF-8/CFC membranes were synthesized through the HoP method for removing various organic dyes, such as Reactive blue 19, RhB, toluidine blue, methylene blue, methyl orange, and crystal violet [169]. Overall, the electrostatic effect allowed the proposed ZIF-8-based membrane to exhibit different adsorption effects on dyes with different charges, e.g., the developed CFC-ZIF-8 membrane achieved relatively higher adsorption efficiency on cationic dyes. However, by modulating the functional groups and the structure of MOFs-coupled-fiber membranes, the adsorption scope of dyes could be expanded. Due to the electrostatic repulsive force between silk and aramid nanofibrils, spider-web-like ZIF-8 fiber membranes were built up through a solvothermal method to optimize the surface structure, and further improve the adsorption efficiency of organic dyes (e.g., methyl violet, Congo red, malachite green, and methylene blue) from water [170]. The hybrid substrate enabled the rejection ratio of more than 99 % of both positively and negatively charged dyes, ascribing to the abundant intermolecular interactions including electrostatic interactions, hydrogen bonding, hydrophobic interactions, etc.

Through the catalytic degradation process, organic dyes with high mole mass can be degraded into smaller molecules, further degraded into water and carbon dioxide, which could be a fundamental solution for organic dye pollution. ZIF-8 is an ideal assistant for the formation of $^{\bullet}OH$ radicals under light irradiation, which are crucial for the photocatalytic process [171]. Mahmoodi *et al.* [172] synthesized α-Fe_2O_3 nanofiber membranes and encrusted ZIF-8 on the fiber via direct solvothermal growth. The optimal percentage of photodegradation for degrading Reactive red 198 was 94 % with the aid of H_2O_2 as shown in Fig. 15**a**. The ZIF-8/Fe_2O_3 composite was stable after recycled utilization at different pH, indicating probability for practical environmental application. MIL-101-NH_2(Fe), which is also one of the effective photocatalytic MOFs working under visible light, was fabricated by ALD-assisted growth on nylon fibers for the degradation of RhB [173]. As shown in Fig. 15**b, c**, the hybrid fiber presented a rugged surface. The concentration of RhB solution decreased by 98.9 % after 2 h of light irradiation. Further experiments confirmed that the principle of RhB removal was the synergy of both adsorption and photocatalysis, in which Fe^{3+} from MIL-101-NH_2(Fe) reacted with H_2O_2, forming $HOO^{\bullet}$ radicals, further degrading RhB into CO_2 and H_2O as shown in Fig. 15**d**. Although the catalytic efficiency of Nylon@Al_2O_3@MOF fiber membranes (98.9 %) was slightly lower compared with that of MIL-101-NH_2(Fe) powder (99.7 %), the recyclability of MOFs-coupled-fiber membranes endowed them with a more practical choice for photocatalytic applications.

Organic dyes are a series of organic contaminants, whose molecular weight and diameter are larger than heavy metal ions. Adsorption and catalytic degradation are common ways for the control of organic dyes. Better adsorption performance can commonly be achieved by enhancing

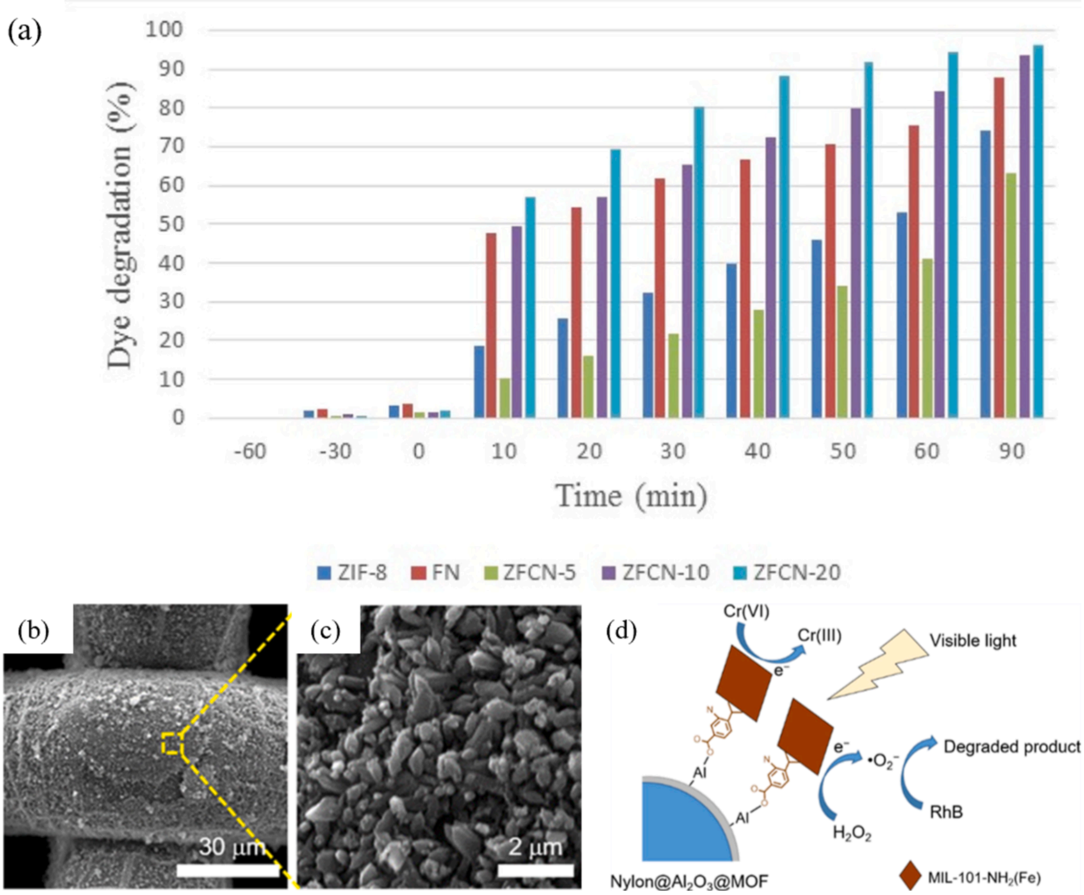

Fig. 15. (a) The percentage of degradation of RR198 using 0.003 g of catalysts at pH = 3, 50 mg/L dye solution[172]; (b, c) Nylon@Al_2O_3@MOF with the magnified image of the surface[173]; (d) Proposed decomposition mechanism of RhB and Cr (VI) on Nylon@ Al_2O_3@MOF[173].

the dispersibility of MOFs. It is also remarkable that the electrostatic interaction between organic dyes and MOFs-coupled-fiber membranes affects the adsorption efficiency since the electronic charges of various organic dyes vary greatly [167]. Furthermore, the MOFs-coupled-fiber membrane with uniform MOF dispersibility also presents proper behavior in catalytic degradation, as adsorption is the prerequisite for catalytic degradation.

3.3. Emerging pollutants

Emerging pollutants (EPs) are characterized as novel substances lacking regulatory status[174–181]. EPs encompass a wide range of man-made chemicals (e.g., antibiotics, persistent organic pollutants (POPs), endocrine disruptors, pharmaceuticals, etc.), which are essential in common life [181]. However, the presence of those contaminants in the aqueous environment has become a global issue. EPs have harmful effects on both human health and aquatic ecosystems even with low concentrations. For example, some pharmaceuticals and endocrine disruptors could imitate natural hormones, therefore impacting the metabolic processes of living [182,183]. In addition, there is a lack of understanding of the medium- and long-term effects of EPs on human health, the environment, and aquatic habitats [174]. Among various kinds of materials for water remediation, MOFs-coupled-fiber membranes performed excellent ability in the removal of EPs. The large specific area of MOFs-coupled-fiber membranes provides abundant contact sites for controlling emerging pollutants, which usually present at a relatively low concentration in water [184]. For the removal of EPs from water, adsorption and catalytic degradation are two main mechanisms.

Antibiotics are extensively used in the agriculture, livestock, and pharmaceutical industries, and are widely detected in water with an active state [185–191]. However, even at low concentrations, antibiotics can also induce antibiotic-resistance genes [191]. Consequently, removing antibiotics from aqueous systems is urgent to protect human health and environmental safety. Adsorption has been proven as one of the most cost-effective methods for the removal of antibiotics [192]. Four types of MOFs (MIL-53(Al), ZIF-8, UiO-66-NH_2, and NH_2-MIL-125 (Ti)) were deposited on PDA-modified electrospun PVA/SiO_2 hybrid nanofiber mats to adsorb chloramphenicol in water [5]. The synthesizing pathways for MIL-53(Al), UiO-66-NH_2, and NH_2-MIL-125(Ti) composites were direct solvothermal growth, and a LbL method was applied for the synthesis of the ZIF-8 composite. The equilibrium adsorption capacities of the MOF composites for chloramphenicol were ZIF-8 (13.9 mg/g) $<$ UiO-66-NH_2 (25.1 mg/g) $<$ NH_2-MIL-125(Ti) (49.5 mg/g) $<$ MIL-53(Al) (79.5 mg/g), corresponding to the BET surface area (17.059, 58.623, 253.209, and 437.973 m^2/g respectively). However, the adsorption efficiency is still inadequate for environmental applications. Mass transmission is crucial since most antibiotics are macromolecules, and the pores of MOFs are nanoscale. Mesoporous ZIF-8/PAN-fiber membranes were constructed for the effective removal of antibiotics with the sacrifice of PVP in substrate fibers in doping during the electrospinning method to accelerate mass transmission [98]. The mesopores could enhance the diffusion of contaminant molecules, improving both the adsorption rate and adsorption capacity. The maximum adsorption capacity of porous ZIF-8/PAN fibers for tetracycline was 885.24 mg/g, which was close to that of pure ZIF-8 (900.90 mg/g) with a loading amount of 71.4 %. The pores could provide abundant MOF-polymer interfaces, which are responsible for the exceptional adsorption capacity as shown in Fig. 16**a**. Electrostatic interaction, π-π interaction, and hydrogen bonds all took part in the tetracycline adsorption (Fig. 16**b**). After 10 adsorption–desorption cycles, the removal efficiency was still above 97 %. Synthesizing MOFs with semiconductor properties onto fiber substrates can efficiently remove antibiotics from water through the synergy effect of photocatalysis and adsorption. For example, Yu *et al.* [57] synthesized CFC/UiO-66-NH_2/BiOBr fibers to remove levofloxacin and ciprofloxacin in water. As shown in Fig. 16**c, d**, after introducing BiOBr to CFC/UiO-66-NH_2 fibers, the degraded efficiency of levofloxacin and ciprofloxacin enhanced to 92.2 % and 86.4 %, respectively. The superior degradation performance could be attributed to the construction of heterojunctions between UiO-66-NH_2 and BiOBr, facilitating the redox reaction to occur under lower potential as shown in Fig. 16**e** [193].

POPs in water have raised concerns about their toxic and unbiodegradable nature [194,195]. Lots of POPs are mutagenic and carcinogenic, harming the nerve and endocrine systems of all the living [196–202]. As a kind of water-stable MOF, UiO-66 was loaded on

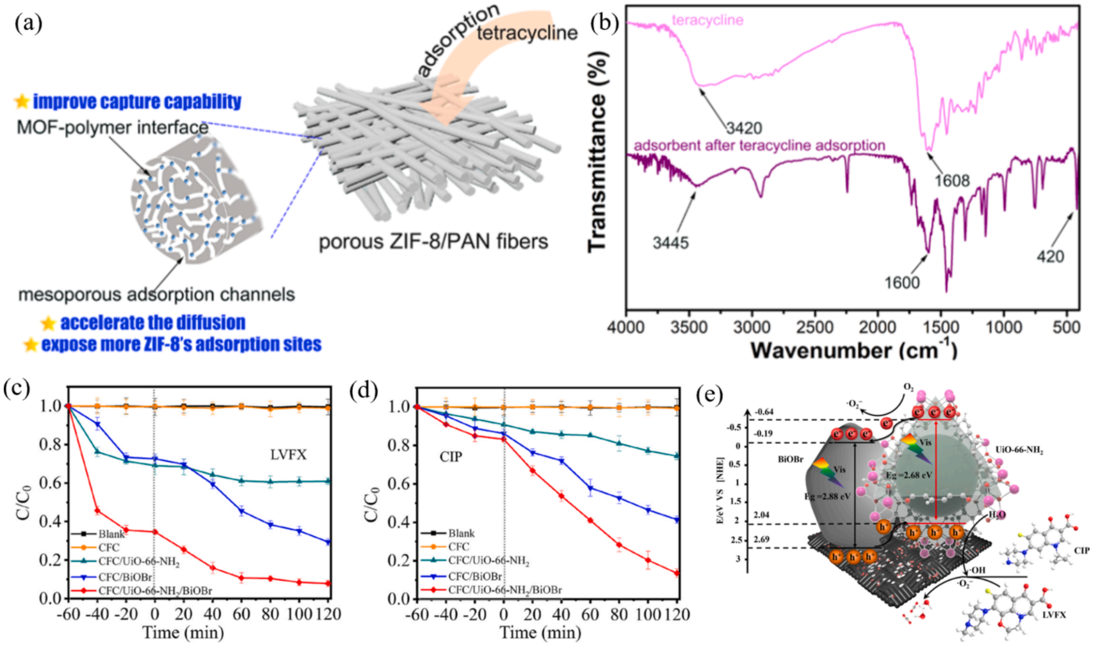

Fig. 16. (a) Proposed effects of constructed mesopores in the fibers for tetracycline adsorption[98]; (b) FTIR spectra of tetracycline and porous ZIF-8/PAN fibers after tetracycline adsorption[98]; (c) Removal efficiency of levofloxacin; (d) Removal efficiency of ciprofloxacin[193]; (e) Proposed mechanism of CFC/UiO-66-NH_2/BiOBr[193].

carboxymethylated cotton fibers through direct solvothermal growth for the adsorption of methylchlorophenoxypropionic acid (a commonly used herbicide) from water [202]. Due to the uniform and dense coating of MOFs on the surface of cotton fiber, the adsorption capacity reached 12.8 mg/g. To eliminate the crisis of POPs ultimately, catalytic degradation should be considered. For example, Hou *et al.* [203] fabricated a lignin/PVA/Co/Fe-MOF fiber membrane with the assistance of electrospinning and direct solvothermal methods for the degradation of perfluorooctanoic acid (PFOA). Under solar light irradiation, $SO_4^{\bullet-}$ and other radicals were rapidly produced by transition metals and photogenerated electrons to activate PMS and $S_2O_8^{2-}$, degrading PFOA consequently. Due to the synergy effect of PMS-AOP and photocatalysis, 89.6 % of PFOA was degraded after 3 h, and the degradation efficiency retained 77 % after 4 cycles.

Because of the structural similarities to natural hormones, endocrine disruptors may interfere with the functioning of endocrine systems in humans[204–207]. TMU-16-NH_2 was loaded on the surface of silk fiber using a LbL strategy for the adsorption of morphine from water[207]. Due to the strong hydrogen bonding interactions between morphine and MOFs, the adsorption capacity was high, and the adsorption process finished within 120 min. Incorporated with catalytic degradation, the high-efficiency removal performance could be accomplished. PMS-based AOP degradation is simple and efficient, which can also be used in the degradation of endocrine disruptors. A Ni/ZIF-8/ZnO-CFC membrane was fabricated for bisphenol A degradation[208]. Aligned ZnO nanorods were grown on the CFC substrate, which served as the zinc source to grow ZIF-8, forming a Ni/ZIF-8/ZnO system ultimately. Under the synergistic adsorption and catalytic degradation, the removal percentage of bisphenol A reached 98.8 % within 30 min, with Ni/ZIF-8/ZnO being a catalyst for PMS activation. The introduction of Ni

Table 1

Summary of the preparation and purification performance of MOFs-coupled-fiber membranes.

MOFs-coupled-fiber Membrane	Preparation			Contaminants removal				Refs.
				Adsorption		Catalytic degradation		
	MOF	Substrate fiber	Preparation method	Contaminants	Capacity (mg/g)	Contaminants	Removal efficiency (%)	
UiO-66-NH_2-PAM-PET	UiO-66-NH_2	PET	Direct solvothermal growth	Pb(II)	711.99	–	–	[149]
ZIF-67/CA	ZIF-67	CA	Direct solvothermal growth	Cu(II)	18.9	–	–	[157]
ZIF-8/Fe_2O_3	ZIF-8	PVA- Fe_3O_4 fiber	Direct solvothermal growth	–	–	Reactive red 198	94	[172]
MIL-53(Al)/PVA/SiO_2	MIL-53 (Al)	PVA/SiO_2	Direct solvothermal growth	chloramphenicol	79.5	–	–	[5]
UiO-66-NH_2/PVA/ SiO_2	UiO-66-NH_2	PVA/SiO_2	Direct solvothermal growth	chloramphenicol	25.1	–	–	[5]
NH_2-MIL-125(Ti)/ PVA/SiO_2	NH_2-MIL-125(Ti)	PVA/SiO_2	Direct solvothermal growth	chloramphenicol	49.5	–	–	[5]
CFC/UiO-66-NH_2/ BiOBr	UiO-66-NH_2	CFC	Direct solvothermal growth	–	–	Levofloxacin, ciprofloxacin	92.2, 86.4	[57]
UiO-66/Cotton	UiO-66	Cotton	Direct solvothermal growth	methylchlorophenoxypropionic acid	12.8	–	–	[202]
Lignin/PVA/Co/Fe-MOF	Co/Fe MOFs	Lignin/PVA	Direct solvothermal growth	–	–	Perfluorooctanoic acid (PFOA)	89.6	[203]
Ni/ZIF-8/ZnO-CFC	ZIF-8	CFC	Direct solvothermal growth	–	–	Bisphenol A	98.8	[208]
Nylon-6@UiO-66-NH_2	UiO-66-NH_2	Nylon	Seed-assisted secondary growth	Cr(VI)	202.79	Cr(VI)	100	[139]
ZIF-8/PVA/SiO_2	ZIF-8	PVA/SiO_2	Layer-by-layer method	chloramphenicol	13.9	–	–	[5]
Nylon@Al_2O_3@MIL-101-NH_2(Fe)	MIL-101-NH_2(Fe)	Nylon@Al_2O_3	ALD-assisted growth	–	–	Cr(VI), RhB	99.6, 98.9	[173]
UiO-66/PAN	UiO-66	PAN	Doping during electrospinning	As(III), As(V)	32.90, 42.17	–	–	[128]
MOF-808/PVDF/GO	MOF-808	PVDF/GO	Doping during electrospinning	As(V)	180	–	–	[129]
Fe-MOF/PAN	Fe-MOF	PAN	Doping during electrospinning	Cr(VI)	127.70	Cr(VI)	–	[138]
Sb-TBC/PVA	Sb-TBC	PVA	Doping during electrospinning	Pb(II)	194	–	–	[148]
Mesoporous ZIF-8/ PAN	ZIF-8	PAN	Doping during electrospinning	tetracycline	885.24	–	–	[98]
MIL-88A(Fe)/Cotton	MIL-88A (Fe)	Cotton	Covalent immobilization coating	As(III), As(V), ROX, ASA	126.5, 164.0, 261.4, 427.5	–	–	[130]

improved both the adsorption capacity and the activation efficiency of PMS. Based on the composite membrane, a continuous-flow catalytic unit was constructed. After testing for 900 min, the removal capability of bisphenol remains at 98.8 %, which is feasible in environmental applications.

In an aqueous environment, the relatively low concentration of EPs makes it difficult to the removal with the use of membranes. Therefore, MOFs-coupled-fiber membranes with abundant specific surface area could be highly efficient in the control of EPs. Furthermore, most EPs are macromolecules, which could be filtered by the nanostructure in MOFs-coupled-fiber membranes[158,160]. However, EPs with large molecular weight and diameter may block the pores, hindering the mass transmission in adsorption and catalytic degradation. Therefore, the design of the proper pore diameters of different types of MOFs is essential. For the selection of fabricating strategy for MOFs-coupled-fiber membranes, those methods exposing more MOFs to the pollutants are more favorable, including direct solvothermal growth, LbL growth, HoP strategy, and covalent immobilization coating.

In this section, MOFs-coupled-fiber membranes participate in water purification is discussed comprehensively. The summary of the preparation and purification performance of MOFs-coupled-fiber membranes is shown in Table 1. The structure of MOFs-coupled-fiber membranes could be tuned to further enhance the purification capacity by regulating the preparation strategy.

4. Current challenges and future chances

MOFs-coupled-fiber membranes exhibit excellent performance in water purification. Embedding MOFs on fiber-based membranes can avoid agglomeration of MOF particles, expand the contact area between MOFs and pollutants, enhance reaction sites, and thus achieve better water purification performance. To prepare MOFs-coupled-fiber membranes, three main categories of strategies can be adopted based on the formation of MOFs, such as conventional solvothermal synthesis, unconventional synthesis, and preparation of composite materials using pre-synthesized MOFs. The combination of MOF particles and fibers, as well as the comprehensive characteristics exhibited, can be effectively applied to the removal of heavy metal ions, organic dyes, and emerging pollutants in water environmental systems. However, there are still several shortcomings in the development of composite membrane and their applications.

First, although fibrous membranes provide support for loading MOFs, excessive MOF incorporation to fibers can result in the agglomeration phenomenon, which influences mechanical properties. How to balance the high load of MOFs and mechanical properties of MOFs-coupled-fiber membranes has become a difficulty. Therefore, desired fabrication methods can be chosen to grow MOF layers on the fiber surface to increase the loading of MOFs and endow the composite membrane with efficient pollutant control performance.

Second, the improvement of water treatment performance by MOFs-coupled-fiber membranes is relatively easy to achieve, but the existing discussions on the relationship between MOFs-coupled-fiber membranes and the performance of the pollutant treatment are mostly empirical. How to select and precisely regulate the components and structure of MOFs-coupled-fiber membranes to achieve optimal performance has become a challenge. With the rapid development of electronic, computer, and information science, it should be considered to combine these new technologies with the analysis mechanism of MOFs-coupled-fiber membranes. For instance, computational chemistry has emerged as an integral component of modern chemistry, which can determine structures at the molecular level and predict structural optimizations that exhibit enhanced performance in desired applications.

There still exists a major challenge for the practical application of MOFs-coupled-fiber membranes, as it is limited by several issues such as stability, cost, and membrane fouling. First, the prerequisite for using MOF fiber membranes in the practical application is their stability. However, several types of MOFs could decompose in aqueous solutions, limiting their persistence in water purification applications. Further research is needed on how to maintain the long-term stability of MOFs-coupled-fiber membranes in harsh environments such as acidic/alkaline environments, high temperatures, and complex organic solvent systems. Second, membrane fouling of MOFs-coupled-fiber membranes is a fatal problem in practical applications, which has been rarely studied. The cost of MOFs-coupled-fiber membranes also restricts their practical applicability. The synthesis of industrial MOFs-coupled-fiber membranes not only consumes a large amount of high-purity chemical reagents, but also involves complex fabrication processes during the functionalization process that are difficult to implement in industrial production. Therefore, the cost reduction and simplification of the manufacturing process are both necessary to be considered.

Besides, the development of MOFs-coupled-fiber membranes typically requires organic solvents, which may pose a great threat to the environment. Therefore, it is necessary to consider green chemistry to achieve more environmentally friendly MOFs-coupled-fiber systems. Also, the final disposal of MOFs-coupled-fiber membranes should be considered, such as using biodegradable fiber substrates to reduce environmental risks.

Declaration of competing interest

The authors declare that they have no known competing financial interests or personal relationships that could have appeared to influence the work reported in this paper.

Acknowledgements

This work was supported by the Natural Science Foundation of Jiangsu Province of China (BK20220863).

Data availability

Data will be made available on request.

References

[1] Joint News Release. Billions of people will lack access to safe water, sanitation and hygiene in 2030 unless progress quadruples - warn WHO, UNICEF. 2021.

[2] Q. Gu, H.Y. Ng, D. Zhao, J. Wang, Metal-Organic Frameworks (MOFs)-boosted filtration membrane technology for water sustainability, APL Mater. 8 (2020) 040902.

[3] G.R. Xu, Z.H. An, K. Xu, Q. Liu, R. Das, H.L. Zhao, Metal organic framework (MOF)-based micro/nanoscaled materials for heavy metal ions removal: the cutting-edge study on designs, synthesis, and applications, Coord. Chem. Rev. 427 (2021) 213554.

[4] J. Feng, H. Sun, B. Yu, X. Yang, L. Xu, P. Liu, X. Cui, Preparation of NH2-MIL-101 (Fe)@Viscose spunlaced nonwoven porous carbon material for organic dye adsorption, Fibers Polym. 24 (6) (2023) 1983–1994.

[5] A. Li, M. Zhou, P. Luo, J. Shang, P. Wang, L. Lyu, Deposition of MOFs on polydopamine-modified electrospun polyvinyl alcohol/silica nanofibers mats for chloramphenicol adsorption in water, Nano 15 (4) (2020) 2050046.

[6] V.S. Kislik, Liquid Membranes: Principles and Applications in Chemical Separations and Wastewater Treatment, Elsevier, 2009.

[7] S. Qiu, M. Xue, G. Zhu, Metal-organic framework membranes: from synthesis to separation application, Chem. Soc. Rev. 43 (16) (2014) 6116–6140.

[8] M. Golpour, M. Pakizeh, Preparation and characterization of New PA-MOF/PPSU-GO membrane for the separation of KHI from water, Chem. Eng. J. 345 (2018) 221–232.

[9] S. Li, W. Han, Q.F. An, K.T. Yong, M.J. Yin, Defect engineering of MOF-based membrane for gas separation, Adv. Funct. Mater. 33 (38) (2023) 2303447.

[10] Q. Qian, P.A. Asinger, M.J. Lee, G. Han, K. MizrahiRodriguez, S. Lin, F. M. Benedetti, A.X. Wu, W.S. Chi, Z.P. Smith, MOF-based membranes for gas separations, Chem. Rev. 120 (16) (2020) 8161–8266.

[11] J. Li, H. Wang, X. Yuan, J. Zhang, J.W. Chew, Metal-organic framework membranes for wastewater treatment and water regeneration, Coord. Chem. Rev. 404 (2020) 2131166.

[12] Q. Wang, D. Astruc, State of the art and prospects in metal-organic framework (MOF)-based and MOF-derived nanocatalysis, Chem. Rev. 120 (2) (2020) 1438–1511.

[13] R. Freund, O. Zaremba, G. Arnauts, R. Ameloot, G. Skorupskii, M. Dincă, A. Bavykina, J. Gascon, A. Ejsmont, J. Goscianska, M. Kalmutzki, U. Lächelt,

E. Ploetz, C.S. Diercks, S. Wuttke, The current status of MOF and COF applications, Angew. Chem. Int. Ed. 60 (45) (2021) 23975–24001.
[14] Y. Bian, C. Chen, R. Wang, S. Wang, Y. Pan, B. Zhao, C. Chen, L. Zhang, Effective removal of particles down to 15 nm using scalable metal-organic framework-based nanofiber filters, Appl. Mater. Today 20 (2020) 100653.
[15] H. Molavi, A. Hakimian, A. Shojaei, M. Raeiszadeh, Selective dye adsorption by highly water stable metal-organic framework: long term stability analysis in aqueous media, Appl. Surf. Sci. 445 (2018) 424–436.
[16] M.J. Neufeld, J.L. Harding, M.M. Reynolds, Immobilization of metal-organic framework copper(II) benzene-1,3,5-tricarboxylate (CuBTC) onto cotton fabric as a nitric oxide release catalyst, ACS Appl. Mater. Interfaces 7 (48) (2015) 26742–26750.
[17] E. Zanchetta, L. Malfatti, R. Ricco, M.J. Styles, F. Lisi, C.J. Coghlan, C.J. Doonan, A.J. Hill, G. Brusatin, P. Falcaro, ZnO as an efficient nucleating agent for rapid, room temperature synthesis and patterning of Zn-based metal-organic frameworks, Chem. Mater. 27 (3) (2015) 690–699.
[18] M. Molco, F. Laye, E. Samperio, S. ZivSharabani, V. Fourman, D. Sherman, M. Tsotsalas, C. Wöll, J. Lahann, A. Sitt, Performance fabrics obtained by in situ growth of metal-organic frameworks in electrospun fibers, ACS Appl. Mater. Interfaces 13 (10) (2021) 12491–12500.
[19] J. Zhao, M.D. Losego, P.C. Lemaire, P.S. Williams, B. Gong, S.E. Atanasov, T. M. Blevins, C.J. Oldham, H.J. Walls, S.D. Shepherd, M.A. Browe, G.W. Peterson, G.N. Parsons, Highly adsorptive, MOF-functionalized nonwoven fiber mats for hazardous gas capture enabled by atomic layer deposition, Adv. Mater. Interfaces 1 (4) (2014) 1400040.
[20] O. Shekhah, J. Liu, R.A. Fischer, C. Wöll, MOF thin films: existing and future applications, Chem. Soc. Rev. 40 (2) (2011) 1081–1106.
[21] H. Zhang, W. Zhao, M. Zou, Y. Wang, Y. Chen, L. Xu, H. Wu, A. Cao, 3D, mutually embedded MOF@carbon nanotube hybrid networks for high-performance lithium-sulfur batteries, Adv. Energy Mater. 8 (19) (2018) 1800013.
[22] Y. Chen, X. Huang, S. Zhang, S. Li, S. Cao, X. Pei, J. Zhou, X. Feng, B. Wang, Shaping of metal-organic frameworks: from fluid to shaped bodies and robust foams, J. Am. Chem.Soc. 138 (34) (2016) 10810–10813.
[23] F. Zhang, N. Li, J.F. Shi, Y.Y. Wang, D.X. Yan, Z.M. Li, Cation bimetallic MOF anchored carbon fiber for highly efficient microwave absorption, Small 20 (32) (2024) 2312135.
[24] J. Gong, W. Luo, Y. Zhao, J. Wang, S. Wang, C. Hu, J. Yang, Y. Dai, Surface engineering of Ni wires and rapid growth strategy of Ni-MOF synergistically contribute to high-performance fiber-shaped aqueous battery, Small 18 (42) (2022) 2204346.
[25] L. Du, B. Zhang, W. Deng, Y. Cheng, L. Xu, L. Mai, Hierarchically self-assembled MOF network enables continuous ion transport and high mechanical strength, Adv. Energy Mater. 12 (24) (2022) 2200501.
[26] A. Li, J. Xiong, Y. Liu, L. Wang, X. Qin, J. Yu, Fiber-intercepting-particle structured MOF fabrics for simultaneous solar vapor generation and organic pollutant adsorption, Chem. Eng. J. 428 (2022) 131365.
[27] D.T. Lee, Z. Dai, G.W. Peterson, M.G. Hall, N.L. Pomerantz, N. Hoffman, G. N. Parsons, Highly breathable chemically protective MOF-fiber catalysts, Adv. Funct. Mater. 32 (6) (2022) 2108004.
[28] K. Ma, K.B. Idrees, F.A. Son, R. Maldonado, M.C. Wasson, X. Zhang, X. Wang, E. Shehayeb, A. Merhi, B.R. Kaafarani, T. Islamoglu, J.H. Xin, O.K. Farha, Fiber composites of metal-organic frameworks, Chem. Mater. 32 (17) (2020) 7120–7140.
[29] J. Xiong, A. Li, Y. Liu, L. Wang, X. Qin, J. Yu, Scalable and hierarchically designed MOF fabrics by netting MOFs into nanofiber networks for high-performance solar-driven water purification, J. Mater. Chem. A 9 (37) (2021) 21005–21012.
[30] B. Mohan, K. Singh, R.K. Gupta, A. Kumar, A.J.L. Pombeiro, P. Ren, Water purification advances with metal-organic framework-based materials for micro/nanoplastic removal, Sep. Purif. Technol. 343 (2024) 126987.
[31] W. Zhu, M. Han, D. Kim, Y. Zhang, G. Kwon, J. You, C. Jia, J. Kim, Facile preparation of nanocellulose/Zn-MOF-based catalytic filter for water purification by oxidation process, Environ. Res. 205 (2022) 112417.
[32] M. Fu, X. Deng, S.-Q. Wang, F. Yang, L.-C. Lin, M.J. Zaworotko, Y. Dong, Scalable robust nano-porous zr-based MOF adsorbent with high-capacity for sustainable water purification, Sep. Purif. Technol. 288 (2022) 120620.
[33] C. Wang, P. Cheng, Y. Yao, Y. Yamauchi, X. Yan, J. Li, J. Na, In-situ fabrication of nanoarchitectured MOF filter for water purification, J. Hazard. Mater. 392 (2020) 122164.
[34] L. Fei, C. Chen, L. Shen, Y. Zhang, B. Wang, J. Xu, B. Li, S. Raza, H. Lin, Graphene oxide assisted assembly of superhydrophilic MOF-based membrane with 2D/3D hybrid nanochannels for enhanced water purification, Chem. Eng. J. 460 (2023) 141694.
[35] M.S. Attia, A.O. Youssef, M.N. Abou-Omar, E.H. Mohamed, R. Boukherroub, A. Khan, T. Altalhi, M.A. Amin, Emerging advances and current applications of nanoMOF-based membranes for water treatment, Chemosphere 292 (2022) 133369.
[36] X. Zhao, Y. Jiang, T. Wang, Q. Lu, K. Zhao, J. Pan, Photothermal-photocatalytic route of MOF-based membrane with nanosheet array structures for solar-driven water purification, Chem. Eng. J. 475 (2023) 146268.
[37] H. Xu, S. Chen, Y.F. Zhao, F. Wang, F. Guo, MOF-based membranes for remediated application of water pollution, ChemPlusChem 89 (8) (2024) e202400027.
[38] J. Ma, X. Guo, Y. Ying, D. Liu, C. Zhong, Composite ultrafiltration membrane tailored by MOF@GO with highly improved water purification performance, Chem. Eng. J. 313 (2017) 890–898.
[39] F. Liu, W. Li, Y. Liang, X. Zhang, D. Ji, H. Liang, M. Yuan, Y. Zhao, H. Tang, X. Li, J. He, W. Shao, Solution blow spinning ultrafine fiber sponge-loaded MOF-808 for effective adsorption and degradation of mustard gas, ACS Appl. Mater. Interfaces 16 (12) (2024) 15298–15307.
[40] Q. Li, Y. Sun, G. Li, X. Yang, X. Zuo, Enhancing interfacial and electromagnetic interference shielding properties of carbon fiber composites via the hierarchical assembly of the MWNT/MOF interphase, Langmuir 38 (46) (2022) 14277–14289.
[41] S. Dong, H. Niu, L. Sun, S. Zhang, D. Wu, Z. Yang, M. Xiang, Highly dense Ni-MOF nanoflake arrays supported on conductive graphene/carbon fiber substrate as flexible microelectrode for electrochemical sensing of glucose, J. Electroanal. Chem. 911 (2022) 116219.
[42] H.H. Do, C.C. Nguyen, D.L.T. Nguyen, S.H. Ahn, S.Y. Kim, L.Q. Van, MOF-derived NiSe2 nanoparticles grown on carbon fiber as a binder-free and efficient catalyst for hydrogen evolution reaction, Int. J. Hydrogen Energy 47 (98) (2022) 41587–41595.
[43] X. Cai, L. Gao, J. Wang, D. Li, MOF-integrated hierarchical composite fiber for efficient daytime radiative cooling and antibacterial protective textiles, ACS Appl. Mater. Interfaces 15 (6) (2023) 8537–8545.
[44] Z. Zhou, M. Shang, Z. Yao, J. Zhang, Eu-MOF fluorescent fiber detector based on polyacrylonitrile: a highly selective and sensitive luminescence sensor for trace amounts of Fe3+, Dyes Pigm. 198 (2022) 110016.
[45] J. Chen, J. Zheng, F. Wang, Q. Huang, G. Ji, Carbon fibers embedded with FeIII-MOF-5-derived composites for enhanced microwave absorption, Carbon 174 (2021) 509–517.
[46] Y. Dou, W. Zhang, A. Kaiser, Electrospinning of metal-organic frameworks for energy and environmental applications, Adv. Sci. 7 (3) (2020) 1902590.
[47] B.N. Bhadra, P.W. Seo, N.A. Khan, S.H. Jhung, Hydrophobic cobalt-ethylimidazolate frameworks: phase-pure syntheses and possible application in cleaning of contaminated water, Inorg. Chem. 55 (21) (2016) 11362–11371.
[48] L.S. Lai, Y.F. Yeong, K.K. Lau, A.M. Shariff, Effect of synthesis parameters on the formation of ZIF-8 under microwave-assisted solvothermal, Procedia Eng. 148 (2016) 35–42.
[49] Y. Ban, Y. Li, X. Liu, Y. Peng, W. Yang, Solvothermal synthesis of mixed-ligand metal-organic framework ZIF-78 with controllable size and morphology, Microporous Mesoporous Mater. 173 (2013) 29–36.
[50] D. Hu, X. Song, S. Wu, X. Yang, H. Zhang, X. Chang, M. Jia, Solvothermal synthesis of co-substituted phosphomolybdate acid encapsulated in the UiO-66 framework for catalytic application in olefin epoxidation, Chin. J. Catal. 42 (2) (2021) 356–366.
[51] M. Fiaz, M. Athar, S. Rani, M. Najam-ul-Haq, M.A. Farid, One pot solvothermal synthesis of Co3O4@UiO-66 and CuO@UiO-66 for improved current density towards hydrogen evolution reaction, Mater. Chem. Phys. 239 (2020) 122320.
[52] S. Bae, N. Zaini, K.S.N. Kamarudin, K.S. Yoo, J. Kim, M.R. Othman, Rapid solvothermal synthesis of microporous UiO-66 particles for carbon dioxide capture, Korean J. Chem. Eng. 35 (3) (2018) 764–769.
[53] S. Hu, M. Liu, K. Li, Y. Zuo, A. Zhang, C. Song, G. Zhang, X. Guo, Solvothermal synthesis of NH2-MIL-125(Ti) from circular plate to octahedron, CrstEngComm 16 (41) (2014) 9645–9650.
[54] B. Tan, Y. Luo, X. Liang, S. Wang, X. Gao, Z. Zhang, Y. Fang, Mixed-solvothermal synthesis of MIL-101(Cr) and its water adsorption/desorption performance, Ind. Eng. Chem. Res. 58 (8) (2019) 2983–2990.
[55] C. Zhang, L. Ai, J. Jiang, Solvothermal synthesis of MIL–53(Fe) hybrid magnetic composites for photoelectrochemical water oxidation and organic pollutant photodegradation under visible light, J. Mater. Chem. A 3 (6) (2015) 3074–3081.
[56] B. Böhringer, R. Fischer, M.R. Lohe, M. Rose, S. Kaskel, P. Küsgens. Metal-Organic Frameworks: Applications from Catalysis to Gas Storage. John Wiley and Sons. 2011.
[57] W. Yu, J. Zhang, Y. Xiong, Z. Wan, J. Zhu, Y. Zhang, Construction of UiO-66-NH2/BiOBr heterojunctions on carbon fiber cloth as macroscale photocatalyst for purifying antibiotics, J.CleanProd. 415 (2023) 137603.
[58] X. Li, T. Liu, Y. Zhang, J. Cai, M. He, M. Li, Z. Chen, L. Zhang, Growth of BiOBr/ZIF-67 nanocomposites on carbon fiber cloth as filter-membrane-shaped photocatalyst for degrading pollutants in flowing wastewater, Adv. Fiber Mater. 4 (6) (2022) 1620–1631.
[59] F. Luo, X. Liang, W. Chen, S. Wang, X. Gao, Z. Zhang, Y. Fang, Bimetallic MOF-derived solar-triggered monolithic adsorbent for enhanced atmospheric water harvesting, Small 19 (48) (2023) 2304477.
[60] M. Toriello, M. Afsari, H.K. Shon, L.D. Tijing, Progress on the fabrication and application of electrospun nanofiber composites, Membranes 10 (9) (2020) 204.
[61] C. Liu, Y. Wu, C. Morlay, Y. Gu, B. Gebremariam, X. Yuan, F. Li, general deposition of metal-organic frameworks on highly adaptive organic-inorganic hybrid electrospun fibrous substrates, ACS Appl. Mater. Interfaces 8 (4) (2016) 2552–2561.
[62] Z. Wu, Z. Chen, J. Chen, X. Ning, P. Chen, H. Jiang, H. Qiu, Enhanced adsorption and synergistic photocatalytic degradation of tetracycline by MOF-801/GO composites via solvothermal synthesis, Environ. Sci.: Nano 9 (12) (2022) 4609–4618.
[63] W. Zhang, Z. Shahnavaz, X. Yan, X. Huang, S. Wu, H. Chen, J. Pan, T. Li, J. Wang, One-step solvothermal synthesis of raspberry-like NiCo-MOF for high-performance flexible supercapacitors for a wide operation temperature range, Inorg. Chem. 61 (38) (2022) 15287–15301.
[64] S.R. Ahrenholtz, C.C. Epley, A.J. Morris, Solvothermal preparation of an electrocatalytic metalloporphyrin MOF thin film and its redox hopping charge-transfer mechanism, J. Am. Chem. Soc. 136 (6) (2014) 2464–2472.
[65] S. Gee, B. Johnson, A.L. Smith, Optimizing electrospinning parameters for piezoelectric PVDF nanofiber membranes, J. Memb. Sci. 563 (2018) 804–812.

[66] H. Katepalli, M. Bikshapathi, C.S. Sharma, N. Verma, A. Sharma, Synthesis of hierarchical fabrics by electrospinning of PAN nanofibers on activated carbon microfibers for environmental remediation applications, Chem. Eng. J. 171 (3) (2011) 1194–1200.

[67] A.X. Lu, A.M. Ploskonka, T.M. Tovar, G.W. Peterson, J.B. Decoste, Direct surface growth of UIO-66-NH2 on polyacrylonitrile nanofibers for efficient toxic chemical removal, Ind. Eng.Chem.Res. 56 (49) (2017) 14502–14506.

[68] D. Ji, S. Peng, L. Fan, L. Li, X. Qin, S. Ramakrishna, Thin MoS2 nanosheets grafted MOFs-derived porous Co-N-C flakes grown on electrospun carbon nanofibers as self-supported bifunctional catalysts for overall water splitting, J. Mater. Chem. A 5 (45) (2017) 23898–23908.

[69] X. Zhang, Y. Sun, Y. Liu, Z. Zhai, S. Guo, L. Peng, Y. Qin, C. Li, UiO-66-NH2Fabrics: role of trifluoroacetic acid as a modulator on MOF uniform coating on electrospun nanofibers and efficient decontamination of chemical warfare agent simulants, ACS Appl. Mater. Interfaces 13 (33) (2021) 39976–39984.

[70] K. Ma, T. Islamoglu, Z. Chen, P. Li, M.C. Wasson, Y. Chen, Y. Wang, G. W. Peterson, J.H. Xin, O.K. Farha, Scalable and template-free aqueous synthesis of zirconium-based metal-organic framework coating on textile fiber, J. Am. Chem. Soc. 141 (39) (2019) 15626–15633.

[71] F. Ahmadijokani, H. Molavi, A. Bahi, R. Fernández, P. Alaee, S. Wu, S. Wuttke, F. Ko, M. Arjmand, Metal-organic frameworks and electrospinning: a happy marriage for wastewater treatment, Adv. Funct. Mater. 32 (51) (2022) 2207723.

[72] Q. Zhang, Z. Li, H. Dai, L. Zhang, J. Zhang, Y. Liu, J. Lin, K. Liang, Y. Ying, Y. Li, Y. Fu, Biomineralization-mimetic growth of ultrahigh-load metal-organic frameworks on inert glass fibers to prepare hybrid membranes for collecting organic hazards in unconventional environment, Chem. Eng. J. 430 (2022) 132956.

[73] Z. Li, G. Zhou, H. Dai, M. Yang, Y. Fu, Y. Ying, Y. Li, Biomineralization-mimetic preparation of hybrid membranes with ultra-high loading of pristine metal-organic frameworks grown on silk nanofibers for hazard collection in water, J. Mater. Chem. A 6 (8) (2018) 3402–3413.

[74] Y. Zhang, Y. Zhang, X. Wang, J. Yu, B. Ding, Ultrahigh metal-organic framework loading and flexible nanofibrous membranes for efficient CO2 capture with long-term, ultrastable recyclability, ACS Appl. Mater. Interfaces 10 (40) (2018) 34802–34810.

[75] Y. Xu, Y. Wen, W. Zhu, Y.N. Wu, C. Lin, G. Li, Electrospun nanofibrous mats as skeletons to produce MOF membranes for the detection of explosives, Mater. Lett. 87 (2012) 20–23.

[76] Y. Bian, Z. Niu, S. Wang, Y. Pan, L. Zhang, C. Chen, Removal of size-dependent submicron particles using metal-organic framework-based nanofiber air filters, ACS Appl. Mater. Interfaces 14 (20) (2022) 23570–23576.

[77] Y. Bian, Z. Niu, C. Zhang, Y. Pan, Y. Wang, C. Chen, Encrusting MOF nanoparticles onto nanofibers via spray-initiated synthesis to boost the filtration performances of nanofiber membranes, Sep. Purif. Technol. 331 (2024) 125569.

[78] Y. Bian, R. Wang, S. Wang, C. Yao, W. Ren, C. Chen, L. Zhang, Metal-organic framework-based nanofiber filters for effective indoor air quality control, J. Mater. Chem. A 6 (32) (2018) 15807–15814.

[79] W. Liu, H. Zhang, W. Zhang, M. Wang, J. Li, Y. Zhang, H. Li, Surface modification of a polylactic acid nanofiber membrane by zeolitic imidazolate framework-8 from secondary growth for drug delivery, J. Mater. Sci. 55 (31) (2020) 15275–15287.

[80] Y. Chen, S. Zhang, S. Cao, S. Li, F. Chen, S. Yuan, C. Xu, J. Zhou, X. Feng, X. Ma, B. Wang, Roll-to-roll production of metal-organic framework coatings for particulate matter removal, Adv. Mater. 29 (2017) 1606221.

[81] H. Wang, X. Zhang, R. Yao, S. Zhao, P. Zhao, R. Yang, L. Wang, Y. Huang, T. Wei, X. Li, Z. Fan, B. Wang, In situ rapid versatile method for the preparation of zirconium metal-organic framework filters, Sci. China Chem. 65 (12) (2022) 2462–2467.

[82] D.K. Yoo, H.C. Woo, S.H. Jhung, Removal of particulate matter with metal-organic framework-incorporated materials, Coord. Chem. Rev. 422 (2020) 213477.

[83] Y. Chen, S. Li, X. Pei, J. Zhou, X. Feng, S. Zhang, Y. Cheng, H. Li, R. Han, B. Wang, A solvent-free hot-pressing method for preparing metal-organic-framework coatings, Angew. Chem. Int. Edit. 55 (10) (2016) 3419–3423.

[84] L. Peng, X. Zhang, Y. Sun, Y. Xing, C. Li, Heavy metal elimination based on metal organic framework highly loaded on flexible nanofibers, Environ. Res. 188 (2020) 109742.

[85] A. Wang, R. Fan, X. Zhou, S. Hao, X. Zheng, Y. Yang, Hot-pressing method to prepare imidazole-based Zn(II) metal-organic complexes coatings for highly efficient air filtration, ACS Appl. Mater. Interfaces 10 (11) (2018) 9744–9755.

[86] J. Zhao, B. Gong, W.T. Nunn, P.C. Lemaire, E.C. Stevens, F.I. Sidi, P.S. Williams, C.J. Oldham, H.J. Walls, S.D. Shepherd, M.A. Browe, G.W. Peterson, M.D. Losego, G.N. Parsons, Conformal and highly adsorptive metal-organic framework thin films via layer-by-layer growth on ALD-coated fiber mats, J. Mater. Chem. A 3 (4) (2015) 1458–1464.

[87] L. Lu, C. Hu, Y. Zhu, H. Zhang, R. Li, Y. Xing, Multi-functional finishing of cotton fabrics by water-based layer-by-layer assembly of metal-organic framework, Cellul. 25 (7) (2018) 4223–4238.

[88] K. Mi, L. Song, H. Nie, T. Liu, X. Li, Layer-by-layer growth of ZIF-8 on electrospun carbon nanofiber membranes for high-performance supercapacistor electrode, J. Energy Chem. 47 (8) (2020) 221–224.

[89] T.C.F. Silva, Y. Habibi, J.L. Colodette, T. Elder, L.A. Lucia, A fundamental investigation of the microarchitecture and mechanical properties of tempo-oxidized nanofibrillated cellulose (NFC)-based aerogels, Cellul. 19 (6) (2012) 1945–1956.

[90] Z. Li, N. Hori, A. Takemura, Synthesis and characterization of Cu-BTC metal-organic frameworks onto lignocellulosic fibers by layer-by-layer method in aqueous solution, Cellul. 27 (3) (2020) 1733–1744.

[91] S. Khanjani, A. Morsali, Ultrasound-promoted coating of MOF-5 on silk fiber and study of adsorptive removal and recovery of hazardous anionic Dye “Congo Red”, Ultrason Sonochem. 21 (4) (2014) 1424–1429.

[92] A.R. Abbasi, K. Akhbari, A. Morsali, Dense coating of surface mounted CuBTC metal-organic framework nanostructures on silk fibers, prepared by layer-by-layer method under ultrasound irradiation with antibacterial activity, Ultrason. Sonochem. 19 (4) (2012) 846–852.

[93] H.F. Barton, A.K. Davis, D.T. Lee, G.N. Parsons, Solvothermal synthesis of MIL-96 and UiO-66-NH2 on atomic layer deposited metal oxide coatings on fiber, Mats. 136 (2018) e57734.

[94] D. Zacher, A. Baunemann, S. Hermes, R.A. Fischer, Deposition of microcrystalline [Cu3(Btc)2] and [Zn2(Bdc)2(Dabco)] at alumina and silica surfaces modified with patterned self assembled organic monolayers: evidence of surface selective and oriented growth, J. Mater. Chem. 17 (27) (2007) 2785–2792.

[95] C. Wang, H. Wang, R. Luo, C. Liu, J. Li, X. Sun, J. Shen, W. Han, L. Wang, Metal-organic framework one-dimensional fibers as efficient catalysts for activating peroxymonosulfate, Chem. Eng. J. 330 (2017) 262–271.

[96] Y. Zhang, S. Yuan, X. Feng, H. Li, J. Zhou, B. Wang, Preparation of nanofibrous metal-organic framework filters for efficient air pollution control, J. Am. Chem. Soc. 138 (18) (2016) 5785–5788.

[97] S. An, J.S. Lee, B.N. Joshi, H.S. Jo, K. Titov, J.S. Chang, C.H. Jun, S.S. Al-Deyab, Y.K. Hwang, J.C. Tan, S.S. Yoon, Freestanding fiber mats of zeolitic imidazolate framework 7 via one-step, scalable electrospinning, J. Appl. Polym. Sci. 133 (32) (2016) 43788.

[98] R. Zhao, X. Shi, T. Ma, H. Rong, Z. Wang, F. Cui, G. Zhu, C. Wang, Constructing mesoporous adsorption channels and MOF-polymer interfaces in electrospun composite fibers for effective removal of emerging organic contaminants, ACS Appl. Mater. Interfaces 13 (1) (2021) 755–764.

[99] S.A. Torres-Cortés, M. Velasquez, L.D. Pérez, C.A. Sierra, Ex situ synthesis of MOF@PET/cotton textile fibers as potential antibacterial materials, J.Polym.Res. 29 (10) (2022) 427.

[100] M. Yu, W. Li, Z. Wang, B. Zhang, H. Ma, L. Li, J. Li, Covalent immobilization of metal-organic frameworks onto the surface of nylon - a new approach to the functionalization and coloration of textiles, Sci. Rep. 6 (2016) 22796.

[101] D.T. Lee, J. Zhao, G.W. Peterson, G.N. Parsons, Catalytic, “MOF-Cloth” formed via directed supramolecular assembly of UiO-66-NH2 crystals on atomic layer deposition-coated textiles for rapid degradation of chemical warfare agent simulants, Chem. Mater. 29 (11) (2017) 4894–4903.

[102] L. Jiao, Y. Wang, H.L. Jiang, Q. Xu, Metal-organic frameworks as platforms for catalytic applications, Adv. Mater. 30 (37) (2018) 1703663.

[103] R. Peng, S. Zhang, Y. Yao, J. Wang, X. Zhu, R. Jiang, J. Zhang, W. Zhang, C. Wang, MOFs meet electrospinning: new opportunities for water treatment, Chem. Eng. J. 453 (2023) 139669.

[104] H. Furukawa, F. Gándara, Y.-B. Zhang, J. Jiang, W.L. Queen, M.R. Hudson, O. M. Yaghi, Water adsorption in porous metal-organic frameworks and related materials, J. Am. Chem. Soc. 136 (11) (2014) 4369–4381.

[105] H. Furukawa, K.E. Cordova, M. O'Keeffe, O.M. Yaghi, The chemistry and applications of metal-organic frameworks, Science 341 (6149) (2013) 1230444.

[106] J. Li, X. Wang, G. Zhao, C. Chen, Z. Chai, A. Alsaedi, T. Hayat, X. Wang, Metal-organic framework-based materials: superior adsorbents for the capture of toxic and radioactive metal ions, Chem. Soc. Rev. 47 (7) (2018) 2322–2356.

[107] X. Ma, Y. Chai, P. Li, B. Wang, Metal-organic framework films and their potential applications in environmental pollution control, Acc. Chem. Res. 52 (5) (2019) 1461–1470.

[108] L. Järup, Hazards of heavy metal contamination, Br. Med. Bull. 68 (1) (2003) 167–182.

[109] K. Yin, Q. Wang, M. Lv, L. Chen, Microorganism remediation strategies towards heavy metals, Chem. Eng. J. 360 (2019) 1553–1563.

[110] A.P. Lim, A.Z. Aris, A review on economically adsorbents on heavy metals removal in water and wastewater, Rev. Environ. Sci. Biotechnol. 13 (2014) 163–181.

[111] M. Bilal, I. Ihsanullah, M. Younas, M. Ul Hassan Shah, Recent advances in applications of low-cost adsorbents for the removal of heavy metals from water: a critical review, Sep. Purif. Technol. 278 (2021) 119510.

[112] L.S. Miranda, B. Wijesiri, G.A. Ayoko, P. Egodawatta, A. Goonetilleke, Water-Sediment interactions and mobility of heavy metals in aquatic environments, Water Res. 202 (2021) 117386.

[113] P.A. Kobielska, A.J. Howarth, O.K. Farha, S. Nayak, Metal-organic frameworks for heavy metal removal from water, Coord. Chem. Rev. 358 (2018) 92–107.

[114] C. Zamora-Ledezma, D. Negrete-Bolagay, F. Figueroa, E. Zamora-Ledezma, M. Ni, F. Alexis, V.H. Guerrero, Heavy metal water pollution: a fresh look about hazards, novel and conventional remediation methods, Environ. Technol. Innov. 22 (2021) 101504.

[115] S. Bolisetty, M. Peydayesh, R. Mezzenga, Sustainable technologies for water purification from heavy metals: review and analysis, Chem. Soc. Rev. 48 (2) (2019) 463–487.

[116] L. Joseph, B.-M. Jun, J.R.V. Flora, C.M. Park, Y. Yoon, Removal of heavy metals from water sources in the developing world using low-cost materials: a review, Chemosphere 229 (2019) 142–159.

[117] N. Abdollahi, G. Moussavi, S. Giannakis, A review of heavy metals' removal from aqueous matrices by metal-organic frameworks (MOFs): state-of-the art and recent advances, J. Environ. Chem. Eng. 10 (3) (2022) 107394.

[118] A. Chakraborty, S. Bhattacharyya, A. Hazra, A.C. Ghosh, T.K. Maji, Post-synthetic metalation in an anionic MOF for efficient catalytic activity and removal of heavy metal ions from aqueoussolution, Chem.Commun. 52 (13) (2016) 2831–2834.
[119] F. Ahmadijokani, S. Tajahmadi, A. Bahi, H. Molavi, M. Rezakazemi, F. Ko, T. M. Aminabhavi, M. Arjmand, Ethylenediamine-functionalized Zr-based MOF for efficient removal of heavy metal ions from water, Chemosphere 264 (2021) 128466.
[120] J.E. Efome, D. Rana, T. Matsuura, C.Q. Lan, Effects of operating parameters and coexisting ions on the efficiency of heavy metal ions removal by nano-fibrous metal-organic framework membrane filtration process, Sci. Total Environ. 674 (2019) 355–362.
[121] S. Lata, S.R. Samadder, Removal of arsenic from water using nano adsorbents and challenges: a review, J. Environ. Manage. 166 (2016) 387–406.
[122] H. Lu, Z. Zhu, H. Zhang, J. Zhu, Y. Qiu, L. Zhu, S. Küppers, Fenton-like catalysis and oxidation/adsorption performances of acetaminophen and arsenic pollutants in water on a multimetal Cu–Zn–Fe-LDH, ACS Appl. Mater. Interfaces 8 (38) (2016) 25343–25352.
[123] M. Zhang, K. Wan, J. Zeng, W. Lin, C. Ye, X. Yu, Co-selection and stability of bacterial antibiotic resistance by arsenic pollution accidents in source water, Environ. Int. 135 (2020) 105351.
[124] M.K. Murthy, P. Khandayataray, C.S. Mohanty, R. Pattanayak, A review on arsenic pollution, toxicity, health risks, and management strategies using nanoremediation approaches, Rev. Environ. Health 39 (2) (2024) 269–289.
[125] J.M. McArthur, P.K. Sikdar, M.A. Hoque, U. Ghosal, Waste-water impacts on groundwater: Cl/Br ratios and implications for arsenic pollution of groundwater in the Bengal Basin and Red River Basin, Vietnam, Sci. Total Environ. 437 (2012) 390–402.
[126] J. Bundschuh, J. Schneider, M.A. Alam, N.K. Niazi, I. Herath, F. Parvez, B. Tomaszewska, L.R.G. Guilherme, J.P. Maity, D.L. López, A.F. Cirelli, A. Pérez-Carrera, N. Morales-Simfors, M.T. Alarcón-Herrera, P. Baisch, D. Mohan, A. Mukherjee, Seven potential sources of arsenic pollution in latin america and their environmental and health impacts, Sci. Total Environ. 780 (2021) 146274.
[127] Z. Wang, P. Luo, X. Zha, C. Xu, S. Kang, M. Zhou, D. Nover, Y. Wang, Overview assessment of risk evaluation and treatment technologies for heavy metal pollution of water and soil, J. Clean Prod. 379 (2022) 134043.
[128] Q. Guo, Y. Li, X.Y. Wei, L.W. Zheng, Z.Q. Li, K.G. Zhang, C.G. Yuan, Electrospun metal-organic frameworks hybrid nanofiber membrane for efficient removal of As (III) and As(V)fromwater, Ecotoxicol. Environ. Saf. 228 (2021) 112990.
[129] L. Kong, Y. Wang, C.B. Andrews, C. Zheng, One-step construction of hierarchical porous channels on electrospun MOF/polymer/graphene oxide composite nanofibers for effective arsenate removal from water, Chem. Eng. J. 435 (2022) 134830.
[130] D. Pang, C.C. Wang, P. Wang, W. Liu, H. Fu, C. Zhao, Superior removal of inorganic and organic arsenic pollutants from water with MIL-88A(Fe) decorated on cotton fibers, Chemosphere 254 (2020) 126829.
[131] M.H. Dehghani, M.M. Taher, A.K. Bajpai, B. Heibati, I. Tyagi, M. Asif, S. Agarwal, V.K. Gupta, Removal of noxious Cr (VI) ions using single-walled carbon nanotubes and multi-walled carbon nanotubes, Chem. Eng. J. 279 (2015) 344–352.
[132] I. Koc, H. Cobanoglu, U. Canturk, K. Key, S. Kulac, H. Sevik, Change of Cr concentration from past to present in areas with elevated air pollution, Int. J. Environ. Sci. Technol. 21 (2) (2024) 2059–2070.
[133] S. Prasad, K.K. Yadav, S. Kumar, N. Gupta, M.M.S. Cabral-Pinto, S. Rezania, N. Radwan, J. Alam, Chromium contamination and effect on environmental health and its remediation: a sustainable approaches, J. Environ. Manage. 285 (2021) 112174.
[134] C. He, L. Gu, Z. Xu, H. He, G. Fu, F. Han, B. Huang, X. Pan, Cleaning chromium pollution in aquatic environments by bioremediation, photocatalytic remediation, electrochemical remediation and coupled remediation systems, Environ. Chem. Lett. 18 (2020) 561–576.
[135] C.-H. Tseng, C. Lei, Y.-C. Chen, Evaluating the health costs of oral hexavalent chromium exposure from water pollution: a case study in Taiwan, J. Clean. Prod. 172 (2018) 819–826.
[136] M. Yoshinaga, H. Ninomiya, M.M.A. Al Hossain, M. Sudo, A.A. Akhand, N. Ahsan, M.A. Alim, Md. Khalequzzaman, M. Iida, I. Yajima, N. Ohgami, M. Kato, A comprehensive study including monitoring, assessment of health effects and development of a remediation method for chromium pollution, Chemosphere 201 (2018) 667–675.
[137] X. He, P. Li, Surface Water Pollution in the Middle Chinese Loess Plateau with Special Focus on Hexavalent Chromium (Cr6+): Occurrence, Sources and Health Risks, Expo. Health 12 (3) (2020) 385–401.
[138] S. Miao, J. Guo, Z. Deng, J. Yu, Y. Dai, Adsorption and reduction of Cr(VI) in water by iron-based metal-organic frameworks (Fe-MOFs) composite electrospun nanofibrous membranes, J. Clean Prod. 370 (2022) 133566.
[139] W. Ji, X. Wang, T. Ding, S. Chakir, Y. Xu, X. Huang, H. Wang, Electrospinning preparation of nylon-6@UiO-66-NH2 fiber membrane for selective adsorption enhanced photocatalysis reduction of Cr(VI) in water, Chem. Eng. J. 451 (2023) 138973.
[140] A.T. Paulino, L.B. Santos, J. Nozaki, Removal of Pb2+, Cu2+, and Fe3+ from battery manufacture wastewater by chitosan produced from silkworm chrysalides as a low-cost adsorbent, React. Funct. Polym. 68 (2) (2008) 634–642.
[141] J. Moros, I. Llorca, M.L. Cervera, A. Pastor, S. Garrigues, M. de la Guardia, Chemometric determination of arsenic and lead in untreated powdered red paprika by diffuse reflectance near-infrared spectroscopy, Anal.Chim.Acta 613 (2) (2008) 196–206.
[142] S. Kumar, M.A. Rahman, M.R. Islam, M.A. Hashem, M.M. Rahman, Lead and other elements-based pollution in soil, crops and water near a lead-acid battery recycling factory in bangladesh, Chemosphere 290 (2022) 133288.
[143] S. Zhou, Z. Yuan, Q. Cheng, Z. Zhang, J. Yang, Rapid in situ determination of heavy metal concentrations in polluted water via portable XRF: using Cu and Pb as example, Environ. Pollut. 243 (2018) 1325–1333.
[144] H. Cheng, Y. Hu, Lead (Pb) isotopic fingerprinting and its applications in lead pollution studies in china: a review, Environ. Pollut. 158 (5) (2010) 1134–1146.
[145] A. El Azhari, A. Rhoujjati, M.L. El Hachimi, J. Ambrosi, Pollution and ecological risk assessment of heavy metals in the soil-plant system and the sediment-water column around a former Pb/Zn-mining area in NE Morocco, Ecotoxicol. Environ. Saf. 144 (2017) 464–474.
[146] E. Siddiqui, J. Pandey, Assessment of heavy metal pollution in water and surface sediment and evaluation of ecological risks associated with sediment contamination in the ganga river: a basin-scale study, Environ. Sci. Pollut. Res. 26 (11) (2019) 10926–10940.
[147] V. Kumar, A. Sharma, R. Kumar, R. Bhardwaj, A. Kumar Thukral, J. Rodrigo-Comino, Assessment of Heavy-Metal Pollution in Three Different Indian Water Bodies by Combination of Multivariate Analysis and Water Pollution Indices, Hum. Ecol. Risk Assess. 26 (1) (2020) 1–16.
[148] N.D. Shooto, C.W. Dikio, D. Wankasi, L.M. Sikhwivhilu, F.M. Mtunzi, E.D. Dikio, Novel PVA/MOF nanofibres: fabrication, evaluation and adsorption of lead ions from aqueous solution, Nanoscale. Res. Lett. 11 (1) (2016) 414.
[149] F. Zhao, C. Su, W. Yang, Y. Han, X. Luo, C. Li, W. Tang, T. Yue, Z. Li, In-situ growth of UiO-66-NH2 onto polyacrylamide-grafted nonwoven fabric for highly efficient Pb(II) removal, Appl. Surf. Sci. 527 (2020) 146862.
[150] H. Demiral, C. Güngör, Adsorption of copper(II) from aqueous solutions on activated carbon prepared from grape bagasse, J. Clean Prod. 124 (2016) 103–113.
[151] H. Genç-Fuhrman, P. Wu, Y. Zhou, A. Ledin, Removal of As, Cd, Cr, Cu, Ni and Zn from polluted water using an iron based sorbent, Desalination 226 (2007) 357–370.
[152] G. Izydorczyk, K. Mikula, D. Skrzypczak, K. Moustakas, A. Witek-Krowiak, K. Chojnacka, Potential environmental pollution from copper metallurgy and methods of management, Environ. Res. 197 (2021) 111050.
[153] M.A. Ahsan, V. Jabbari, A.A. El-Gendy, M.L. Curry, J.C. Noveron, ultrafast catalytic reduction of environmental pollutants in water via MOF-derived magnetic Ni and Cu nanoparticles encapsulated in porous carbon, Appl. Surf. Sci. 497 (2019) 143608.
[154] D. Qiao, G. Wang, X. Li, S. Wang, Y. Zhao, Pollution, sources and environmental risk assessment of heavy metals in the surface AMD water, sediments and surface soils around unexploited Rona Cu Deposit, Tibet, China, Chemosphere 248 (2020) 125988.
[155] F.W.B. Bugenyi, Copper pollution studies in Lakes George and Edward, Uganda: The Distribution of Cu, Cd and Fe in the Water and Sediments, Environ. Pollut. B. 3 (2) (1982) 129–138.
[156] V. Kertész, G. Bakonyi, B. Farkas, Water pollution by Cu and Pb can adversely affect mallard embryonic development, Ecotoxicol. Environ. Saf. 65 (1) (2006) 67–73.
[157] X. Hou, H. Zhou, J. Zhang, Y. Cai, F. Huang, Q. Wei, High adsorption pearl-necklace-like composite membrane based on metal-organic framework for heavy metal ion removal, Part. Part. Syst. Char. 35 (6) (2018) 1700438.
[158] R.K. Gautam, M. Goswami, R.K. Mishra, P. Chaturvedi, M.K. Awashthi, R.S. Singh, B.S. Giri, A. Pandey, Biochar for remediation of agrochemicals and synthetic organic dyes from environmental samples: a review, Chemosphere 272 (2021) 129917.
[159] N. Buvaneswari, C. Kannan, Plant toxic and non-toxic nature of organic dyes through adsorption mechanism on cellulose surface, J. Hazard. Mater. 189 (1) (2011) 294–300.
[160] V. Vinayagam, K.N. Palani, S. Ganesh, S. Rajesh, V.V. Akula, R. Avoodaiappan, O. S. Kushwaha, A. Pugazhendhi, Recent developments on advanced oxidation processes for degradation of pollutants from wastewater with focus on antibiotics and organic dyes, Environ. Res. 240 (2024) 117500.
[161] A. Rafiq, M. Ikram, S. Ali, F. Niaz, M. Khan, Q. Khan, M. Maqbool, Photocatalytic degradation of dyes using semiconductor photocatalysts to clean industrial water pollution, J. Ind. Eng. Chem. 97 (2021) 111–128.
[162] M. Cao, Y. Shen, Z. Yan, Q. Wei, T. Jiao, Y. Shen, Y. Han, Y. Wang, S. Wang, Y. Xia, T. Yue, Extraction-like removal of organic dyes from polluted water by the graphene oxide/PNIPAM composite system, Chem. Eng. J. 405 (2021) 126647.
[163] Y. Zhou, M. Elchalakani, H. Liu, B. Briseghella, C. Sun, Photocatalytic concrete for degrading organic dyes in water, Environ. Sci. Pollut. Res. 29 (26) (2022) 39027–39040.
[164] M. Hasanpour, M. Hatami, Photocatalytic performance of aerogels for organic dyes removal from wastewaters: review study, J. Mol. Liq. 309 (2020) 113094.
[165] S. Yadav, K. Shakya, A. Gupta, D. Singh, A.R. Chandran, A. Varayil Aanappalli, K. Goyal, N. Rani, K. Saini, A review on degradation of organic dyes by using metal oxide semiconductors, Environ. Sci. Pollut. R. 30 (28) (2023) 71912–71932.
[166] U. Shanker, M. Rani, V. Jassal, Degradation of Hazardous Organic Dyes in Water by Nanomaterials, Environ. Chem. Lett. 15 (2017) 623–642.
[167] A. Tkaczyk, K. Mitrowska, A. Posyniak, Synthetic organic dyes as contaminants of the aquatic environment and their implications for ecosystems: a review, Sci. Total Environ. 717 (2020) 137222.
[168] T. Li, L. Liu, Z. Zhang, Z. Han, Preparation of nanofibrous metal-organic framework filter for rapid adsorption and selective separation of cationic dye from aqueous solution, Sep. Purif. Technol. 237 (2020) 116360.

[169] L. Yin, Z. Liu, Y. Yang, Y. Guo, G. Zhang, F. Gai, Y. Ao, Jieran Liu, B. Xin, Y. Liu, Structured carbon fiber cloth-templated ZIF-8 by binder-free method for efficient dyes removal from water, Mater. Chem. Phys. 242 (2020) 122563.

[170] L. Lv, X. Han, M. Mu, X. Wu, C. Li, Templating metal-organic framework into fibrous nanohybrids for large-capacity and high-flux filtration interception, J. Memb. Sci. 622 (2021) 119049.

[171] H.P. Jing, C.C. Wang, Y.W. Zhang, P. Wang, R. Li, Photocatalytic degradation of methylene blue in ZIF-8, RSC Adv. 4 (97) (2014) 54454–54462.

[172] N.M. Mahmoodi, S. Keshavarzi, M. Oveisi, S. Rahimi, B. Hayati, Metal-organic framework (ZIF-8)/inorganic nanofiber (Fe2O3) nanocomposite: green synthesis and photocatalytic degradation using LED irradiation, J.Mol.Liq. 291 (2019) 111333.

[173] M. Kang, S.H. Yu, K.Y. Baek, M.M. Sung, S. Cho, MIL-101-NH2(Fe)-coated nylon microfibers for immobilized photocatalysts in RhB and Cr(VI) removal, ACS Omega 8 (17) (2023) 15298–15305.

[174] T. Deblonde, C. Cossu-Leguille, P. Hartemann, Emerging pollutants in wastewater: a review of the literature, Int. J. Hyg. Environ. Health 214 (6) (2011) 442–448.

[175] C.S. Tshangana, A.A. Muleja, A.T. Kuvarega, T.J. Malefetse, B.B. Mamba, The applications of graphene oxide quantum dots in the removal of emerging pollutants in water: an overview, J. Water Process Eng. 43 (2021) 102249.

[176] M. Tobajas, C. Belver, J.J. Rodriguez, Degradation of emerging pollutants in water under solar irradiation using novel TiO2-ZnO/clay nanoarchitectures, Chem. Eng. J. 309 (2017) 596–606.

[177] C. Peña-Guzmán, S. Ulloa-Sánchez, K. Mora, R. Helena-Bustos, E. Lopez-Barrera, J. Alvarez, M. Rodriguez-Pinzón, Emerging pollutants in the urban water cycle in latin america: a review of the current literature, J. Environ. Manage. 237 (2019) 408–423.

[178] P.M. Álvarez, J. Jaramillo, F. López-Piñero, P.K. Plucinski, Preparation and characterization of magnetic TiO2 nanoparticles and their utilization for the degradation of emerging pollutants in water, Appl. Catal. B 100 (1) (2010) 338–345.

[179] R. Rodil, J.B. Quintana, E. Concha-Graña, P. López-Mahía, S. Muniategui-Lorenzo, D. Prada-Rodríguez, Emerging pollutants in sewage, surface and drinking water in Galicia (NW Spain), Chemosphere 86 (10) (2012) 1040–1049.

[180] Y. Tang, M. Yin, W. Yang, H. Li, Y. Zhong, L. Mo, Y. Liang, X. Ma, X. Sun, Emerging Pollutants in Water Environment: Occurrence, Monitoring, Fate, and Risk Assessment. Water Environ. Res. 91 (10) (2019) 984–991.

[181] M. Gavrilescu, K. Demnerová, J. Aamand, S. Agathos, F. Fava, Emerging pollutants in the environment: present and future challenges in biomonitoring, ecological risks and bioremediation, New Biotechnol. 32 (1) (2015) 147–156.

[182] M.S. Samuel, K. Venkatesan Savunthari, N. Chandrasekar, R. Balaji, E. Selvarajan, Removal of environmental contaminants of emerging concern using metal-organic framework composite, Environ. Technol. Innov. 25 (2022) 102216.

[183] Q. Chen, Q.W. Chen, C. Zhuang, P.P. Tang, N. Lin, L.Q. Wei, Controlled release of drug molecules in metal-organic framework material HKUST-1, Inorg. Chem. Commun. 79 (2017) 78–81.

[184] X. Du, M. Zhou, Strategies to enhance catalytic performance of metal-organic frameworks in sulfate radical-based advanced oxidation processes for organic pollutants removal, Chem. Eng. J. 403 (2021) 126346.

[185] O. Alegbeleye, O.B. Daramola, A.T. Adetunji, O.T. Ore, Y.J. Ayantunji, R. K. Omole, D. Ajagbe, S.O. Adekoya, Efficient Removal of Antibiotics from Water Resources Is a Public Health Priority: A Critical Assessment of the Efficacy of Some Remediation Strategies for Antibiotics in Water, Environ. Sci. Pollut. R. 29 (38) (2022) 56948–57020.

[186] S. Wu, Y. Lin, Y.H. Hu, Strategies of tuning catalysts for efficient photodegradation of antibiotics in water environments: a review, J. Mater. Chem. A 9 (5) (2021) 2592–2611.

[187] M. Magureanu, D. Piroi, N.B. Mandache, V. David, A. Medvedovici, C. Bradu, V. I. Parvulescu, Degradation of antibiotics in water by non-thermal plasma treatment, Water Res. 45 (11) (2011) 3407–3416.

[188] J. Lyu, L. Yang, L. Zhang, B. Ye, L. Wang, Antibiotics in soil andwaterin china–a systematic review and source analysis, Environ. Pollut. 266 (2020) 115147.

[189] S. Yang, K. Carlson, Routine monitoring of antibiotics in water and wastewater with a radioimmunoassay technique, Water Res. 38 (14) (2004) 3155–3166.

[190] D. Azanu, B. Styrishave, G. Darko, J.J. Weisser, R.C. Abaidoo, Occurrence and risk assessment of antibiotics in water and Lettuce in Ghana, Sci. Total Environ. 622–623 (2018) 293–305.

[191] Y.G. Zhu, T.A. Johnson, J.Q. Su, M. Qiao, G.X. Guo, R.D. Stedtfeld, S. A. Hashsham, J.M. Tiedje, Diverse and abundant antibiotic resistance genes in chinese swine farms, Proc. Natl. Acad. Sci. USA 110 (9) (2013) 3435–3440.

[192] Y. Hong, D. Thirion, S. Subramanian, M. Yoo, H. Choi, H.Y. Kim, J.F. Stoddart, C. T. Yavuz, Precious metal recovery from electronic waste by a porous porphyrin polymer, Proc. Natl. Acad. Sci. 117 (28) (2020) 16174–16180.

[193] M. Peñas-Garzón, M.J. Sampaio, Y.L. Wang, J. Bedia, J.J. Rodriguez, C. Belver, C. G. Silva, J.L. Faria, Solar photocatalytic degradation of parabens using UiO-66-NH2, Sep. Purif. Technol. 286 (2022) 120467.

[194] A.A. Adeyemo, I.O. Adeoye, O.S. Bello, Metal organic frameworks as adsorbents for dye adsorption: overview, prospects and future challenges, Toxicol. Environ. Chem. 94 (2012) 1846–1863.

[195] Y. Pi, X. Li, Q. Xia, J. Wu, Y. Li, J. Xiao, Z. Li, Adsorptive and photocatalytic removal of persistent organic pollutants (POPs) in water by metal-organic frameworks (MOFs), Chem. Eng. J. 337 (2018) 351–371.

[196] M. Trojanowicz, Removal of persistent organic pollutants (POPs) from waters and wastewaters by the use of ionizing radiation, Sci. Total Environ. 718 (2020) 134425.

[197] R. Lohmann, E. Markham, J. Klanova, P. Kukucka, P. Pribylova, X. Gong, R. Pockalny, T. Yanishevsky, C.C. Wagner, E.M. Sunderland, Trends of diverse POPs in air and water across the western atlantic ocean: strong gradients in the ocean but not in the air, Environ. Sci. Technol. 55 (14) (2021) 9498–9507.

[198] Z.L. Zhang, H.S. Hong, J.L. Zhou, J. Huang, G. Yu, Fate and assessment of persistent organic pollutants in water and sediment from minjiang river estuary, Southeast China, Chemosphere 52 (9) (2003) 1423–1430.

[199] J. Aravind kumar, T. Krithiga, S. Sathish, A.A. Renita, D. Prabu, S. Lokesh, R. Geetha, S.K.R. Namasivayam, M. Sillanpaa, Persistent organic pollutants in water resources: fate, occurrence, characterization and risk analysis, Sci. Total Environ. 831 (2022) 154808.

[200] Y. Vasseghian, S. Hosseinzadeh, A. Khataee, E.-N. Dragoi, The concentration of persistent organic pollutants in water resources: a global systematic review, meta-analysis and probabilistic risk assessment, Sci. Total Environ. 796 (2021) 149000.

[201] J.P. Unyimadu, O. Osibanjo, J.O. Babayemi, Selected persistent organic pollutants (POPs) in water of river Niger: occurrence and distribution, Environ. Monit. Assess. 190 (1) (2018) 6.

[202] M. Schelling, M. Kim, E. Otal, J. Hinestroza, Decoration of cotton fibers with a water-stable metal-organic framework (UiO-66) for the decomposition and enhanced adsorption of micropollutants in water, Bioengineering 5 (1) (2018) 14.

[203] C. Hou, W. Chen, L. Fu, S. Zhang, C. Liang, Y. Wang, Efficient degradation of perfluorooctanoic acid by electrospun lignin-based bimetallic MOFs nanofibers composite membranes with peroxymonosulfate under solar light irradiation, Int. J. Biol. Macromol. 174 (2021) 319–329.

[204] C.L.S. Vilela, J.P. Bassin, R.S. Peixoto, Water contamination by endocrine disruptors: impacts, microbiological aspects and trends for environmental protection, Environ. Pollut. 235 (2018) 546–559.

[205] W.T. Vieira, M.B. de Farias, M.P. Spaolonzi, M.G.C. da Silva, M.G.A. Vieira, Removal of endocrine disruptors in waters by adsorption, membrane filtration and biodegradation. A review, Environ. Chem. Lett. (2020) 1113–1143.

[206] H.-S. Chang, K.-H. Choo, B. Lee, S.-J. Choi, The methods of identification, analysis, and removal of endocrine disrupting compounds (EDCs) in water, J. Hazard. Mater. 172 (1) (2009) 1–12.

[207] A.R. Abbasi, J. ad D. Aali, A. Azadbakht, A. Morsali, V. Safarifard, Synthesis and characterization of TMU-16-NH2 metal-organic framework nanostructure upon silk fiber: study of structure effect on morphine and methyl orange adsorption affinity, Fibers Polym. 16 (5) (2015) 1193–1200.

[208] Y. Wang, Y. Ge, R. Wang, Z. Liu, Z. Yin, Z. Yang, F. Liu, W. Yang, MOF-Derived Ni/ZIF-8/ZnO arrays on carbon fiber cloth for efficient adsorption-catalytic oxidation, Small 19 (50) (2023) 2303928.

[209] D. Kim, K.C. Koo, J.H. Park, K. Paeng, W. Lee, Roll-to-roll processing of hybrid MOF and nylon membranes for high efficiency removal of toxic gases, heavy metals, and dyes, ACS Appl. Eng. Mater. 1 (4) (2023) 1220–1228.